


**Research Article**

## Oxidized Low-density Lipoproteins and Lipopolysaccharides Augment Carotid Artery Plaque Vulnerability in Hypercholesterolemic Microswine

Nooti S<sup>1</sup>\*, Rai V<sup>1</sup>\*, Radwan MM<sup>1</sup>, Thankam FG<sup>1</sup>, Singh H<sup>1</sup>, Chatzizisis YS<sup>2</sup>, Agrawal DK<sup>1\*</sup>

### Abstract

Atherosclerosis is a chronic inflammatory disease and hypercholesterolemia is a risk factor. This study aims to compare the potency of lipopolysaccharide (LPS) and oxidized low-density lipoproteins (oxLDL) to induce plaque formation and increase plaque vulnerability in the carotid artery of hypercholesterolemic Yucatan microswine. Atherosclerotic lesions at the common carotid artery junction and ascending pharyngeal artery were induced in hypercholesterolemic Yucatan microswine at 5-6 months of age with balloon angioplasty. LPS or oxLDL were administered intraluminally at the site of injury after occluding the arterial flow temporarily. Pre-intervention ultrasound (US), angiography, and optical coherence tomography (OCT) were done at baseline and just before euthanasia to assess post-op parameters. The images from the US, OCT, and angiography in the LPS and the oxLDL-treated group showed increased plaque formation with features suggestive of unstable plaque, including necrotic core, thin fibrous caps, and a signal poor region more with oxLDL compared to LPS. Histomorphology of the carotid artery tissue near the injury corroborated the presence of severe lesions in both LPS and oxLDL-treated pigs but more in the oxLDL group. Vascular smooth muscle and endothelial cells treated with LPS and oxLDL showed increased folds changes in mRNA transcripts of the biomarkers of inflammation and plaque vulnerability compared to untreated cells. Collectively, the results suggest that angioplasty-mediated intimal injury of the carotid arteries in atherosclerotic swine with local administration of LPS or ox-LDL induces vulnerable plaques compared to angioplasty alone and oxLDL is relatively more potent than LPS in inducing vulnerable plaque.

**Keywords:** Atherosclerosis; Chronic inflammation; Hypercholesterolemic swine; Lipopolysaccharide; Ox-LDL; Plaque stabilization; Vulnerable plaque

### Introduction

Despite an advanced understanding of the biology of atherosclerosis, coronary artery disease (CAD) and cerebrovascular disease (CVD) continue to be in the top 3 leading causes of death worldwide [1]. Ischemic strokes, which are the most common presentation of CVD, are often caused by atherosclerotic emboli from the carotid artery after plaque rupture. Studies over the past two decades have demonstrated “vulnerable plaques” as the cause of most acute coronary syndromes (ACS) and strokes [2]. However, despite extensive interest in the possibility of identifying high-risk atherosclerotic lesions, morphological determinants of plaque vulnerability assessed through novel imaging tools, have demonstrated a poor positive predictive value for

### Affiliation:

<sup>1</sup>Department of Translational Research, Western University of Health Sciences, Pomona, California 91763, USA

<sup>2</sup>Division of Cardiovascular Medicine, Leonard M. Miller School of Medicine University of Miami, Miami, FL 33136, USA

\*Equal contributions

### Corresponding author:

Devendra K. Agrawal, Department of Translational Research, Western University of Health Sciences, 309 E. Second Street, Pomona, California 91766, USA.

**Citation:** Sunil Nooti, Vikrant Rai, Mohamed M Radwan, Finosh G Thankam, Harbinder Singh, Yiannis S Chatzizisis, Devendra K Agrawal. Oxidized Low-density Lipoproteins and Lipopolysaccharides Augment Carotid Artery Plaque Vulnerability in Hypercholesterolemic Microswine. *Cardiology and Cardiovascular Medicine*. 7 (2023): 273-294.

**Received:** June 19, 2023

**Accepted:** July 14, 2023

**Published:** July 26, 2023

identifying future adverse events [3]. Vulnerable plaques are typically characterized by the presence of large plaque burden, necrotic cores, chronic inflammation, decreased VSMCs proliferation, a thin fibrous cap, and positively (or outwardly) remodeled plaque lesions while stable plaques have a thick fibrous cap composed mainly of vascular smooth muscle cells (VSMCs) and extracellular matrix (ECM) enveloping a necrotic lipid-rich core [4,5]. Moreover, vulnerable plaques have thin, highly inflamed, and collagen-poor fibrous caps that contain elevated levels of proteases, including metalloproteinases (MMPs) with dual roles of weakening fibrous cap and facilitating migration and proliferation of VSMCs [6]. Atherosclerosis, a complex chronic inflammatory disease, is characterized by the formation of occlusive atherosclerotic plaques (APs) in the inner wall of arteries through the formation of the fatty streak, atheroma, atheromatous plaque, fibro-atheromatous plaque, followed by vulnerable plaque [7,8]. Recent epidemiological studies [9] suggest that the markers of inflammation such as IL-6 [10] and high-sensitivity C-reactive protein [11] independently predict future major cardiovascular events comparable to low-density lipoprotein (LDL) levels. The chronic inflammatory response in the vessel wall is mediated by foam cells, immune cells including macrophages, dendritic cells, T-lymphocytes, and the local effects of cytokines and growth factors released from infiltrating cells. Chronic inflammation plays a critical role in the development, progression, and instability/vulnerability of atherosclerotic plaques [8,12-16]. We previously reported an increased expression of triggering receptor expressed on myeloid cells (TREM)-1 in symptomatic vs asymptomatic carotid atherosclerotic plaques in humans suggesting a possible role of dendritic cells, macrophages, and inflammatory cytokine TNF- $\alpha$  in plaque vulnerability [14-16]. Macrophages, toll-like receptor-4 (TLR-4), and myeloid differentiation primary response gene 88 (MyD88) signaling are common drivers of low-grade systemic inflammation and the presence of hypercholesterolemia adds to the progression of atherosclerosis [17]. Since the first postulation by Brown and Goldstein [18] that LDL must undergo modifications to be atherogenic, the significance of oxidized LDL (ox-LDL) in initiating the pathogenesis of atherosclerosis involving macrophages (specifically foam cell formation) [19] is well established. Ox-LDL can trigger the activation of endothelial cells (ECs) and promote the expression of adhesion molecules on the cell surface mediating the rolling and adhesion of blood monocytes [20]. LDL is also known to undergo oxidation within the atherosclerotic plaques and high plasma and plaque levels of ox-LDL are correlated with plaque vulnerability and rupture [21]. Here, we studied and compared the effect of locally administered LPS and oxLDL in promoting plaque formation and vulnerability radiologically and histologically by evaluating various markers of inflammation (TREM-1 and TLR-4), and plaque vulnerability such as thrombospondin-1 (TSP-1) [22],

interleukin (IL)-23 [23], matrix metalloproteinase (MMP)-7 [24], and vascular cell adhesion molecule (VCAM)-1 [25,26]. The notion to study the inflammatory aspects in progressing plaque vulnerability is supported by our previous findings that the cellular and molecular mechanisms of atherosclerosis, inflammation, and response to injury are like human carotid endarterectomy specimens [15,16] leading to a direct cause and effect relationship in the vulnerable plaque paradigm for clinical translation. Animal models of atherosclerosis, especially mice, rabbits, and swine have served as valuable tools in understanding etiology and pathophysiology to a great extent and are useful for translational studies. With the limitations in using mice and rabbits due to a difference in anatomy, lipid metabolism, and natural resistance to developing atherosclerosis [27]; the swine model represents the best choice to study the occlusive arterial disease because of similarities in the anatomy, physiology, and lipid metabolism, and a similar pathological response of the human and porcine circulatory system. We have developed a novel clinically relevant high cholesterol diet-fed Yucatan swine model of vulnerable plaques in carotid arteries where imaging techniques such as high-resolution ultrasound (USG), angiography, and optical coherence tomography (OCT) that are used in humans, can be directly applied for the study of vulnerable plaques responsible for symptoms in humans upon disruption of fibrous caps [28, 29]. The US, OCT, and histopathological findings in this study revealed that local administration of LPS or ox-LDL after an intimal injury can induce plaque formation, progression, and vulnerability and that ox-LDL is relatively more potent than LPS.

## Materials and Methods

### Animal model:

Yucatan microswine of 4-6 months old weighing between 15-25 kg purchased from Sinclair Bio-resources (MO, USA) were used for this study. We recruited female pigs since they are less aggressive, safer, and easier to handle than males. Also, the commercially available male pigs are castrated for the safety of the personnel, and castration induces hormonal changes which may be a confounding factor in atherosclerosis studies [30]. All animal work was performed as per the guidelines of the National Institutes of Health and USDA for the care and use of experimental animals. Institutional Animal Care and Use Committees at Creighton University (Protocol #1017) and Western University of Health Sciences (Protocol #R19IACUC026) approved the animal research protocols for this study. To assess the baseline and end-point parameters of the vessel, US, angiogram, and OCT were done before the intervention and before sacrificing the swine, as described below. Microswine were housed in the large animal facilities of Creighton University and Western University of Health Sciences with a 12-hour light and dark cycle at 72°-74°F. The swine were fed with an atherogenic diet purchased from Research Diets Inc (RDI) (NJ, USA) at Sinclair Bio-resources

before being transported to our facility and at our facility during experiments. All microswine were fed the RDI swine diet D17012601, which is a high-cholesterol diet (HC; 51% carbohydrates, 20% protein, 10% fat with 4% cholesterol). For our experiments, the microswine were divided randomly into three experimental groups, angioplasty alone, angioplasty + lipopolysaccharide (LPS), and angioplasty + minimally oxidized low-density lipoprotein (oxLDL), each consisting of 6-7 microswine with similar body weights. In addition to these experimental groups, we included 4 swine to examine the effects of LPS and oxLDL on plaque formation in carotid arteries without intimal injury. These swine were injected with LPS and oxLDL alone without angioplasty (no intimal injury). One swine was included without intervention. Thus, the experimental data in this article include the findings in a total of 25 swine.

### Surgical Procedure:

All surgical procedures were performed at our large animal surgical suites in our vivarium. The artery and vein diameter, intima-media thickness (IMT) peak systolic velocity (PSV), and end-diastolic velocity (EDV) were measured before the intervention, follow up at 3 months after the intervention, and just before sacrificing the swine. Angiography and OCT were done during the intervention and just before sacrificing the swine. For balloon angioplasty, animals were pre-anesthetized by administering an intramuscular (IM) injection of a single dose of acepromazine (1.1 mg/kg) followed by a single dose of ketamine (11-33 mg/kg). The unconsciousness was confirmed by the lack of blinking response, jaw tone, and a decrease in respiratory and heart rate. This was followed with inhalational isoflurane in oxygen, 3-4% for induction, and 1-3% for maintenance of anesthesia. A peripheral intravenous catheter line was placed in the auricular vein for IV fluid and drug administration. A prophylactic pre-operative one-time dose of cefazolin (3-5 mg/kg; IM) was administered. Philips Epic 7 ultrasound system (Philips Medical Systems, Bothell, WA, USA), was used for the acquisition of carotid ultrasound. Briefly, the carotid artery on the side of the intervention was examined with the animal in a supine position with the head turned at a 45° angle to the contralateral side. On the interventional side the proximal, mid, and distal common carotid arteries (CCA), were imaged with grayscale and color doppler ultrasound, the diameter, intima-media thickness (IMT) peak systolic velocity (PSV), and end-diastolic velocity (EDV) were measured. Access to the carotid artery for balloon angioplasty was gained through the femoral artery on either side. The groin was shaved and prepped with betadine and alcohol scrubs, and draped, the femoral vessels were identified, and the femoral artery was punctured with ultrasound guidance. A 4F sheath was introduced followed by a 6F sheath to maintain the vascular access patent for insertion of the guiding catheters typically used for human angiography. A guidewire was advanced using the guiding catheter into the aortic arch and

through the carotid trunk and the common carotid artery under fluoroscopic guidance. A balloon angioplasty catheter (Abbott Vascular, USA) was advanced on the guidewire to reach the bifurcation of the selected common carotid artery (CCA) into ascending pharyngeal artery (APA) and inflated to at least 1.1 times the measured internal diameter by OCT. Then, it was moved up and down briefly to induce intimal injury and plaque formation. In the angioplasty alone group, after intimal injury, the catheter was removed without any further intervention. In the angioplasty + LPS and angioplasty + oxLDL groups, the angioplasty balloon was deflated and retracted. Another Over the Wire (OTW) balloon catheter was introduced (Boston Scientific) towards the distal part of the common carotid artery, below the site of injury, and inflated to just block the arterial flow. Intraluminal administration of 100µg of LPS (from *E. coli* 0111: B4; Sigma Aldrich L5293) or 600µg of oxLDL in 3 ml of phosphate-buffered saline at the site of angioplasty was given through the OTW catheter after removing the guidewire while holding the blood flow by keeping the balloon inflated for 2 minutes to induce unstable plaques. We used a total dose of 100µg in a 25-30kg pig to induce a pro-inflammatory response (dose of LPS to induce an inflammatory response in pigs ranges from 0-5µg/kg) [31] while we used 200µg/ml of oxLDL (total 600µg) injected locally because levels of 510.0±86.1 mg/dL in pigs are associated with accelerated atherosclerosis after angioplasty [32] to induce inflammation and plaque formation. Induction of plaque formation in association with inflammation will enhance plaque size and vulnerability [13,33]. All catheters were removed, and the femoral artery puncture site was pressed using a gauze pad for 15 minutes to stop bleeding and prevent hematoma formation. After completion of the procedure, the animal was extubated after the return of reflexes. During post-operative recovery, the animal was kept under observation until the swine was able to stand and move unassisted. A single dose of analgesic (buprenorphine; 0.01-0.03 mg/kg, IM) was given and during the first few postoperative days, the animals were monitored daily for signs of pain or any other complications.

### Optical coherence tomography (OCT):

The OCT examination was performed just before and after the balloon angioplasty to confirm the intimal injury and just before the necropsy at the end of the experiment. Briefly, after intracarotid administration of diluted nitroglycerin (100µg in 10 ml normal saline), a 0.014-inch guidewire was positioned distally in the APA. Subsequently, the OCT catheter (Dragonfly™ DUO imaging catheter; Abbott USA) was advanced to the distal end of the site of intervention. Iodine contrast media was simultaneously injected during OCT pullback. The entire region of interest was scanned, and the images were analyzed via Light Lab OCT imaging proprietary software (Light Lab Imaging; Abbott). One animal suffered CVA and was euthanized postoperatively as per veterinary directives, while the remaining swine included

in the study didn't suffer any complications post-operatively till the end of the experiment.

#### Tissue harvest:

Euthanasia was performed by intravenous administration of a single dose of euthanasia solution (pentobarbital sodium (85 mg/kg) and phenytoin sodium (11 mg/kg)). Swine was observed for the absence of heartbeat and respiration for at least 10 min before harvesting of tissues. The neck was dissected to retrieve the CCA, the bifurcation of CCA into ECA and APA, and APA was excised. The tissues were harvested in 10% formalin, RNA later as per manufacturer's instruction, and fresh frozen for histology, gene expression, and protein expression studies respectively. For histology, tissues were processed in a tissue processor and embedded in paraffin wax and 5µm section slices were cut with a tungsten carbide knife (Leica™, Germany) in a Leica RM2265 rotary microtome (Leica™, Germany), attached to glass slides, and baked.

#### Hematoxylin and Eosin (H&E) and Movat Pentachrome staining:

H&E staining was performed following the standard protocol in our laboratory. Briefly, the tissue sections on the slides were de-paraffinized, rehydrated in ethanol, rinsed in double-distilled water, and stained with hematoxylin for 45 seconds and with eosin for 30s. The stained sections were mounted with a xylene-based mounting medium and a coverslip was placed over the tissue. A Russell-Movat Pentachrome stain kit was used (Cat no. KTRMPPT from American MasterTech scientific laboratory supplies) for pentachrome staining and the tissue sections were stained following the manufacturer's protocol after deparaffinization and rehydration. We stained at least three adjacent sections from each tissue and three to five images from each section were scanned for analysis using a light microscope (Leica DM6) with a scale of 100µm.

#### Immunohistochemistry:

Immunohistochemistry (IHC) was performed using the peroxidase anti-peroxidase method using a secondary antibody conjugated to horseradish peroxidase (HRP). For immunohistochemistry, the slides were deparaffinized and rehydrated. The antigen retrieval was carried out by heating the slide with 1% citrate buffer (C9999; Sigma) in a steamer for 40 min. After a 30-min cool-down period, the slides were washed with 1x phosphate-buffered saline (PBS) for 5 minutes. The tissue sections were circled with a PAP pen and endogenous peroxidases were blocked with 3% hydrogen peroxide (H1009; Sigma) for 15 min and rinsed again in PBS for 5 minutes. Blocking was done using a blocking solution from the Vectastain Elite ABC kit (Vector Labs) and the tissues were incubated for 1 hour at room temperature. The blocking solution was tipped off and tissue sections were incubated with primary antibodies including anti-TLR4

(ab13556); anti-TREM1 (sc19309); anti-MMP7 (ab232737); anti-VCAM1 (ab106777); anti-Thrombospondin-1 -(ab1823); anti CD14 (sc7328); anti IL-12/23 (MAB9121); anti-CD206 (sc70586); anti-CD86 (ab53004) at an empirically optimized dilution and incubated at 4°C overnight. The next day, the slides were washed 3 times for 5 minutes each with 1X PBS and the slides were incubated with the secondary antibody from the corresponding Vectastain Elite ABC kit for 1 hour at room temperature (RT). The slides were rinsed 3 times with 1x PBS, followed by incubation of the tissue sections with the Vectastain ABC horseradish peroxidase (HRP) for 30 minutes at RT. The tissue sections were then rinsed with 1x PBS followed by incubation with 3,3'-diaminobenzidine (DAB) (34002; Thermo Scientific) for 2 to 5 minutes until the development of brown color. After the DAB had developed sufficiently, slides were washed with water, stained in hematoxylin for 10 seconds, rinsed in running tap water for 5 minutes and mounted with a xylene-based mounting medium. Negative controls were stained using IgG isotypes as well as using only secondary antibodies without using primary antibodies (Figure S1 panels A, B, C, and D). The stained slides were imaged with a Leica DM6 microscope. A minimum of three sections from each swine were stained and three to five images were scanned with a light microscope (Leica DM6) with a scale of 100µm and quantified with Image J (NIH) for average stained intensity and average stained area.

#### Cell culture, oxLDL preparation, RNA extraction, and real-time PCR:

Primary endothelial (ECs) and smooth muscle cells (SMCs) were isolated from the common carotid arteries collected after euthanasia. Briefly, ECs were scraped carefully from the inside surface of the artery and resuspended in an Endothelial cell-specific growth medium (ECM 1001; ScienCell) and grown at 37°C with 5%CO<sub>2</sub> in a humidified incubator. SMCs were isolated after mincing the arteries and digesting with Collagenase I. SMCs were cultured in a smooth muscle cell-specific growth medium (SMCM 1101; ScienCell) and cells up to passage 4 were used. The ox-LDL used in this study was prepared by the controlled oxidation of LDL harvested from the plasma of atherosclerotic pigs using a single-step discontinuous gradient ultracentrifugation method (Figure S1 panel E) following the previously reported protocol [34]. The density gradient was created using potassium bromide (KBr) and the density was adjusted to 1.063 g/mL [using the formula plasma (mL) x 0.0834 = KBr (g)] followed by ultra-centrifugation in a Beckman L8 80M Ultracentrifuge using an SW55 Ti swinging bucket rotor at 100,000g for 24 h. The LDL-containing band was carefully removed, and the lipoprotein concentration was measured by Pierce™ BCA Protein Assay Kit. The dialysis-purified LDL was oxidized using 5µM copper sulfate (CuSO<sub>4</sub>) for two hours and was stopped with EDTA and was further purified

by dialysis to form ox-LDL. The level of oxidation was quantified by TBARS assay using a commercially available kit (Cayman chemical, Cat# 10009055) by strictly following the manufacturer's protocol and was detected to be >2µM. 600µg ox-LDL and 100µg LPS were suspended in PBS and filter sterilized for administering in vivo to the swine or in vitro treatment of primary cell cultures.

Total RNA was extracted using TRIZOL reagent (15596026, Invitrogen, Carlsbad, CA) and 1.5 µg of total RNA was used for cDNA synthesis with ImProm-II Reverse Transcription System from Promega following the manufacturer's instructions. Real-time PCR was carried out using a CFX96 Touch Real-Time PCR Detection System from BioRad. The PCR cycling conditions were 3 min at 95°C for initial denaturation, 40 cycles of 15s at 95°C, and 15s at 55–60°C (according to the primer annealing temperatures) followed by melting curve analysis. Reactions were run in triplicate for three independent experiments. The primers for different genes in swine (Table 1) were obtained from Integrated DNA Technologies (Coralville, IA, USA). Expression data were normalized to the geometric mean of the housekeeping gene GAPDH to control the variability in expression levels. Fold change in the expression of mRNA transcripts relative to controls was determined using the 2<sup>-ΔΔCT</sup> after normalizing the CT values with GAPDH.

**Western Blot analysis:**

To investigate the effects of LPS (100µg/ml) and oxLDL

(600µg/3ml) on various markers of inflammation and plaque instability, we treated VSMCs with LPS and oxLDL for 24 hrs and extracted the protein using RIPA buffer. The 20µg protein was loaded and run on SDS gel (4–15% Mini-PROTEAN TGX Precast Protein Gels, 10-well, 50µl BioRad #4561084) followed by transfer to PVDF (polyvinylidene difluoride) membrane. After blocking for 1 hour with skimmed milk at room temperature, the membrane was incubated with primary antibodies (TLR-4 (NB10056566), TIRAP (ab133332), TSP-1 (ab85762), MMP-7 (ab232737), and β-actin (ab8226)) overnight at 40C and then washed with 1x TBST (tris-buffered saline with 0.1% Tween 20). This was followed by incubating the membrane with a secondary antibody and washed with TBST. The membrane was developed with ECL (Thermo Scientific; SuperSignal West Pico PLUS Chemiluminescent Substrate Catalog number: 34580) and imaged with ChemiDoc (Biorad ChemiDoc MP Imaging System). The images were analyzed using ImageJ.

**Statistical analysis:**

Data are presented as the mean ± SD. Data were analyzed using GraphPad Prism 9. The comparison between two groups for the expression of the protein of interest was performed using Student's t-test while multiple comparisons was done using One-way ANOVA with Bonferroni's posthoc test. A probability (p) value < 0.05 was accepted as statistically significant. \*p < 0.05, \*\*p < 0.01, \*\*\*p < 0.001 and \*\*\*\*p < 0.0001.

**Table 1:** Forward and reverse nucleotide sequence of primers used for PCR in this study.

Gene name	Forward	Reverse
TREM1	5'-CCTGGCAGAAGCTGAATCGT-3'	5'-TGGGATCCTTGGGAGGTTGA-3'
TLR4	5'-GGGTCATGCTTCTCCGGGT-3'	5'-TTTCACATCTGCACGCAAGGG-3'
MyD88	5'-CCATTTCGAGATGACCCCTG-3'	5'-TGCACAAACTGGGTATCGCT-3'
Col1A1	5'-CTGGCCTCCCTGGAATGAAG-3'	5'-CCAGCAGGACCAGCATCT-3'
Col3A1	5'-GCTTTGTGCAAAAGGGGACC-3'	5'-GAGCTGTTGGAGGTTGTGGA-3'
Vimentin	5'-CAGCCGGCAGGTGGAC-3'	5'-AAAGTGCTCTCGGCTTCCTC-3'
TSP1	5'-GGTCTGAGTGGACCTTTGC-3'	5'-TCGCATCTGTTGTTGAGGCT-3'
MMP7	5'-ACAGGCTCAGGGCTATCTCA-3'	5'-TGGCTGGCTTGGGAATAGTG-3'
GAPDH	5'-CGGAGTGAACGGATTTGGCCG-3'	5'-GGAAGTGGCCGTGGGTGGAA-3'
18S	5'-CCCACGGAATCGAGAAAGAG-3'	5'-TTGACGGAAGGGCACCA-3'
TIRAP	5'-CCCTTCCCACAACACCAAGA-3'	5'-ACCAGGGCTTATCACTGTGC-3'
TRAM	5'-TCTTTGCTGAGATGCCGTGT-3'	5'-AAGATTGTCCAGGCAGAGCC-3'
TRIF	5'-AAGGTGGCCAACACCTTCAA-3'	5'-CTTCTCCAAGTGGCTCTGGT-3'
TRAF6	5'-ATGCATCTGGACGCCCTAAG-3'	5'-CCCAGTCTGTACTTTCGTGG-3'
RelA	5'-ACCTGGGGATCCAGTGTGTA-3'	5'-AGGGGTTGTTGTTGGTCTGG-3'
IKB	5'-TCTACTGCCAAGGTGGAGA-3'	5'-ATCCTACAAGGGACCGAGCA-3'
IL-6	5'-TGCAGTCACAGAACGAGTGG-3'	5'-CAGGTGCCCCAGCTACATTAT-3'
TNF-α	5'-CATCTACCTGGGAGGGGTCT-3'	5'-CCAGATAGTCGGGCAGGTTG-3'
TGF-β	5'-CCACCCAGATCCTCCTACC-3'	5'-CAGAATCTGGCCGCAATGG-3'
VCAM-1	5'-GCGAGTCTCCCTGTCTTTC-3'	5'-CGTGGATCTGGTCCCGTTAG-3'

## Results

### Ultrasound Imaging showed increased intima-media thickness in angioplasty with oxLDL group:

There was no significant change in the mean intima-media thickness (IMT) before intervention and at the endpoint in both angioplasty only ( $0.70 \pm 0.16$  mm and  $0.74 \pm 0.27$  mm ( $p=0.7322$ )) and angioplasty + LPS groups ( $0.65 \pm 0.17$  and  $0.66 \pm 0.18$  mm ( $p=0.8767$ )). However, there was a 36% increase in mean IMT at the endpoint compared to preintervention in the angioplasty + oxLDL group ( $0.55 \pm 0.18$  vs  $0.75 \pm 0.29$ ,  $p=0.1573$ ) though not significant (Figure 1 panels A and C). Of note, the pre-op average IMT in the angioplasty + oxLDL group was lower than the other two groups and this might be due to the different batches of animals, however, the IMT in all three groups was within the normal range of 0.28 to 1.00mm [35, 36]. This may also be due to the small sample size and thus, warrants a larger sample size and further analysis. The ultrasound findings in the carotid arteries injected with LPS or oxLDL only without any angioplasty did not show any significant difference and the findings were similar to arteries without any intervention (Figure 2 panels F, G, I, J, M, and N). These results suggest that oxLDL with angioplasty increases IMT more than angioplasty alone or in combination with LPS.

### Optical coherence tomography (OCT):

OCT revealed a prominent effect of oxLDL on plaque vulnerability compared to the LPS group and angioplasty alone. Pre-intervention OCT of the carotid artery of hyperlipidemic microswine showed distinct 3 layers of the artery in the entire vessel circumference in all pigs in all three groups. The mean intimal thickness was 0.03 mm in all three groups (Figure 1 panels B and D). The mean intimal thickness measurement in the angioplasty-only group was  $0.14 \pm 0.07$ mm ( $n=6$ ), and in the angioplasty + LPS group was 0.14 mm ( $n=1$ ). The intimal thickness in the other 5 swine in the LPS group and all swine ( $n=7$ ) in the oxLDL group could not be measured owing to the presence of a large atherosclerotic lesion leading to no clear demarcation between intima and media. There was no significant difference between pre-intervention and endpoint mean diameter in angioplasty only ( $1.96 \pm 0.17$  vs  $1.95 \pm 0.21$  mm) and angioplasty + LPS ( $2.11 \pm 0.18$  vs  $2.05 \pm 0.48$  mm) groups while there was a 12.07% increase in the mean diameter in the angioplasty + oxLDL group ( $2.07 \pm 0.32$  vs  $2.32 \pm 0.41$  mm) (Figure 1 panel D). OCT analysis showed signal-rich eccentric plaque with poorly defined borders suggestive of lipid plaque (5 out of 6 swine) and mixed-signal rich and signal-poor concentric plaque with poor visualization of the 3 layers of the artery (1 out of 6 swine) in the angioplasty alone group. In the angioplasty + LPS group, the OCT analysis was suggestive of the presence of neovascularization (thick signal-rich area with a small zone of high attenuation) in one swine, thick signal-rich plaque (stable plaque) in one swine, white and red

thrombus in one swine each, a signal rich eccentric plaque with low attenuation spots casting a posterior shadow with no clear sign of instability in one swine, and unstable plaque (high attenuation region with low attenuation signal rich fibrous cap with poorly defined borders and low attention mass attached to the luminal surface) in one swine. In the angioplasty + oxLDL group, 3 swine displayed the sign of unstable plaque (with necrotic core, thin fibrous cap at the shoulder, and a signal-poor region with poorly defined margins;  $n=3$ ), a ruptured fibrous cap with bright spots casting posterior shadows ( $n=1$ ) and white thrombus, and two swine with a concentric signal rich plaque with no clear sign of instability ( $n=1$ ) in one swine each (Figure 1 panel B and Figure S2).

The presence of unstable and ruptured plaques in 3 swine and plaque with thrombus formation in one swine in oxLDL treated group compared to 1 plaque with clear criteria of instability and two plaques with thrombus formation in LPS treated group suggests that oxLDL causes more severe lesions. These findings are based on the 6 microswine in LPS treated group and 7 microswine in the oxLDL group. OCT revealed no significant difference between the control group (without any intervention) and the arteries injected with LPS and oxLDL without angioplasty (Figure 2 panels H, K, L, O, and P).

### Hematoxylin and Eosin (H&E) staining revealed increased inflammation and plaque rupture with oxLDL:

H&E staining of the carotid artery junction showed stable plaque ( $n=6$ ; thick fibrous cap) and the presence of transmural inflammation ( $n=1$  of 6) in the angioplasty alone group; stable plaque ( $n=5$  of 6), a vulnerable plaque with rupture and intraplaque hemorrhage ( $n=1$  of 6), dense transmural inflammation ( $n=2$  of 6), focal intimal inflammation ( $n=2$  of 6), and tunica intima thickening ( $n=1$  of 6) in angioplasty + LPS group; while complicated plaque with rupture and thrombus formation ( $n=1$  of 6), thickening of tunica intima ( $n=2$  of 6), and thick fibro-atheromatous plaque ( $n=3$  of 6) in angioplasty + oxLDL group (Figure 3). It was also observed that plaque was localized (involving  $<1/3$ rd intimal lining) in the angioplasty alone group while diffuse involving  $>1/2$  intima lining in the angioplasty + LPS group and  $>2/3$ rd intima in the angioplasty + oxLDL group. The localized plaque in the angioplasty group was thick in one artery (Figure 2 panels A and A') while was thin in other samples (Figure S3). H&E staining of the ascending pharyngeal artery (equivalent to the internal carotid artery) in the angioplasty alone group showed atheromatous plaque with dense inflammation in tunica adventitia ( $n=3$  of 6), thickened tunica intima ( $n=1$  of 6), and focal loss of tunica intima ( $n=1$  of 6). In the angioplasty + LPS group, there was focal intimal inflammation ( $n=1$  of 6), a vulnerable plaque with plaque rupture ( $n=1$  of 6), mild to moderate inflammation in the lesion ( $n=5$  of 6), and the presence of necrotic core ( $n=1$  of 6). In the angioplasty +

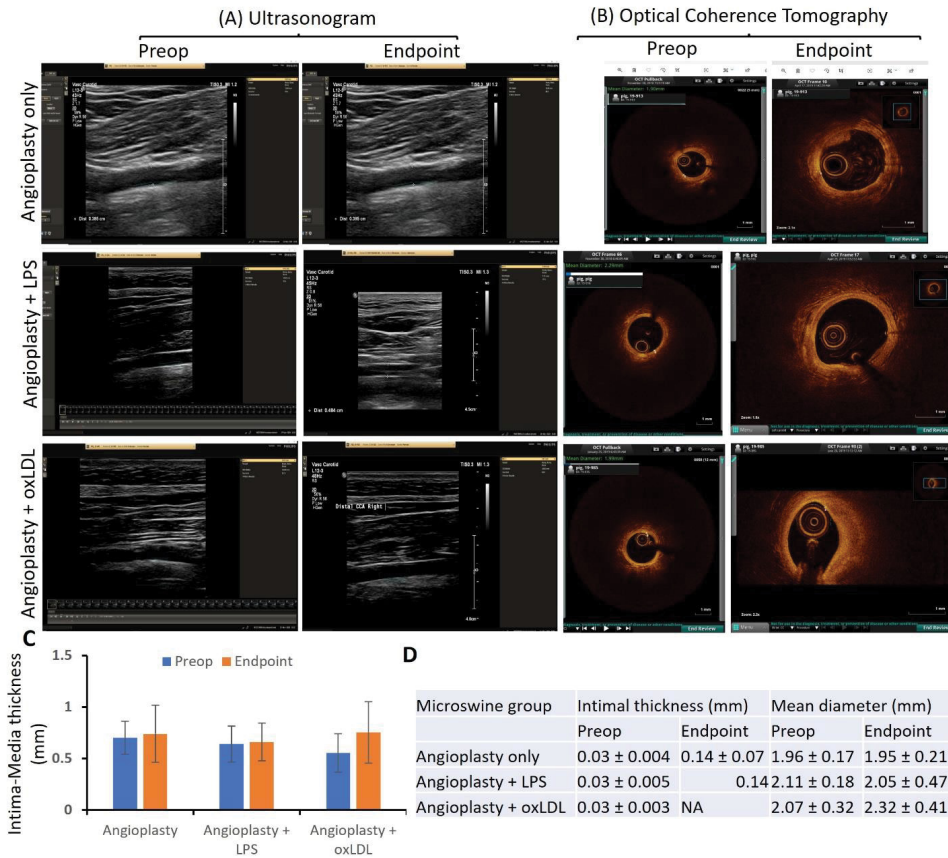


**Figure 1:** Ultrasound and optical coherence tomography (OCT) of carotid arteries. Panel A- preintervention (preop) and before sacrifice (endpoint) representable ultrasound images, panel B- preop and endpoint representable OCT images from all microswine in three groups namely angioplasty only (n=6), angioplasty with lipopolysaccharide (LPS) (n=6), and angioplasty with minimally oxidized low-density lipoprotein (oxLDL) (n=7), panel C- intima-media thickness (IMT) of the common carotid artery, and panel D- intimal thickness and mean diameter of the internal carotid artery. USG images are of the common carotid artery and OCT images were taken in the internal carotid artery. OCT of the carotid vessels before intervention (pre-operative) showed 3 layers of the artery and can be visualized in the entire vessel circumference in all pigs in all three groups, however, the three layers were not demarcated in endpoint OCT because of the atherosclerotic lesion.

oxLDL group, there was intimal thickening (n=2 of 6), dense chronic inflammation (n=3 of 6), and focal stable plaque (n=2 of 6) (Figure 4). There was a presence of intraplaque fibrous tissues in all three groups. H and E staining also revealed the presence of intraplaque lipid deposition with abundance in the angioplasty alone group and mild to moderate in the other two groups in both the carotid junction and ascending pharyngeal artery. Additionally, the presence of blood cells in the plaque suggests the development of vulnerable plaque in the angioplasty + LPS and angioplasty + oxLDL group (Figures 3 and 4). Larger plaques were formed at the carotid junction and internal carotid artery with oxLDL except for one artery where LPS-mediated plaque was larger than in the oxLDL group. Moreover, the presence of a thick fibrous cap in the angioplasty alone group and a thin fibrous cap with endothelium discontinuity in angioplasty + LPS and angioplasty + oxLDL groups suggests induction of instability by LPS and ox-LDL (Figures 3 and 4 and Figure S3).

Additionally, analysis of neo-intimal and plaque area on H & E-stained images of CCA revealed increased NIH +

plaque area (mm<sup>2</sup>) in oxLDL treated group compared to LPS treated and only angioplasty group in the common carotid artery (1.23 ± 1.04 vs 0.88 ± 0.75; p=.000039) and 1.23 ± 1.04 vs 0.75 ± 0.26; p=0.0033) corroborated the US, angiography, and OCT finding. However, for APA in LPS treated group, NIH + plaque area was greater than the angioplasty alone group (0.94 ± 1.34 vs 0.74 ± 0.78; p=0.09). In most of the APA from oxLDL-treated swine, the tissues were fibrosed and thrombosed and the nearby section showed a stenosed lumen (Figure 3 panel C) with lower NIH + plaque area (0.45 ± 0.20) (Figure S1 panel F). This might be due to thrombosis and stenosis post-intervention and oxLDL treatment. Further, H and E-stained sections showed significantly increased IMT in the oxLDL group compared to angioplasty in common carotid (0.74 ± 0.26 vs 0.61 ± 0.12 mm, p=0.003) and increased in LPS compared to angioplasty alone in APA (0.61 ± 0.34 vs 0.52 ± 0.19 mm). IMT in oxLDL was decreased but within the normal range in APA (0.38 ± 0.05mm) (Figure S1 panel G). These results are supportive of our findings of OCT where IMT was not measured due to extensive atherosclerosis and

no clear demarcation between intima and media. The H&E staining of the carotid arteries for control, oxLDL only, and LPS only without angioplasty group revealed normal histomorphology without any neointima or plaque formation (Figures 2 A and C).

**Movat-Pentachrome staining revealed decreased collagens with oxLDL while elastin degradation and fibrosis with LPS:**

The stained slides were semi-quantitatively scored based on the scoring in Table S1 for collagen, fibrin, glycans, and elastin expression. Movat-Pentachrome staining of the carotid junction in the angioplasty alone group (Figure 3 panels D and D') showed a thick fibrous cap with very weak to weak yellow staining for collagen (score of 1-2), minimal blue to weak blue stain for glycans (score of 0-2), very weak to weak red stain for fibrin (score of 1-2), and minimal to very weak purple stain for elastin (score of 0-1) in the intima and media. The angioplasty + LPS group (Figure 3 panels E and E') revealed very weak to weak yellow staining for collagen (score of 1-2), very weak to moderate blue stain for

glycans (a score of 1-3), very weak to moderate red stain for fibrin (score of 1-3), and weak to moderate purple stain for elastin (a score of 2-3). An elastin stain in the angioplasty + LPS group was present in the atherosclerotic plaque lesion as well as in the intima and media. The staining intensity for elastin was more in the media compared to the plaque lesion and one-third to half artery was stained for elastin. The angioplasty + oxLDL group (Figure 3 panels F and F') revealed minimal to weak yellow stain for collagen (a score of 0-2), very weak to moderate blue stain for glycans (a score of 1-3), very weak to strong red stain for fibrin (a score of 1-4), and weak to moderate purple stain for elastin (a score of 2-3). Elastin stain in the angioplasty + oxLDL group was present in the atherosclerotic plaque lesion as well as in the intima and media. The staining intensity for elastin was more in the media compared to the plaque lesion and elastin stain was seen throughout the artery, suggesting increased degraded elastin in the media and the propensity of the artery towards stiffness. Movat-Pentachrome staining in the ascending pharyngeal artery (APA) at the site of the lesion in the angioplasty alone group (Figure 4 panels D and D')

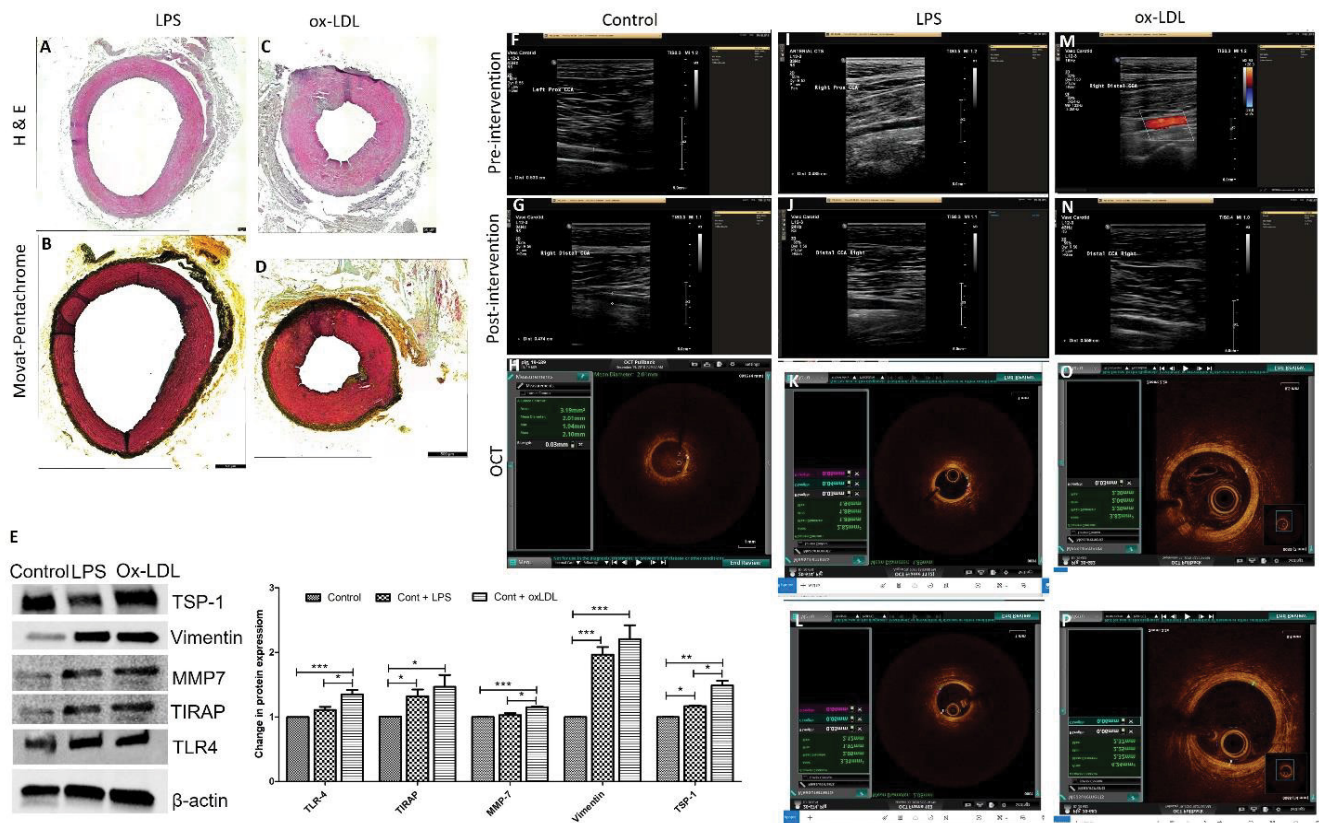


**Figure 2:** Histological, radiological, and molecular results in arteries treated with LPS and oxLDL without angioplasty. Hematoxylin and eosin staining (panels A and C), Movat-Pentachrome staining (panels B and D), Western Blot analysis in VSMCs treated with LPS and ox-LDL (panel E), ultrasound imaging data (panels F, G, J, K, M, and N), and optical coherence tomography (OCT) images (panels H, K, L, O, and P) in LPS and ox-LDL treated carotid arteries. US images are from common carotid arteries while OCT images are from internal carotid arteries (ascending pharyngeal artery). Toll-like receptor-4 (TLR-4), Thrombospondin-1 (TSP-1), TIRAP (Toll-interleukin-1 Receptor (TIR) domain-containing adaptor protein), matrix metalloproteinase-7 (MMP-7), thrombospondin (TSP)-1, lipopolysaccharides (LPS), oxidized low-density lipoprotein (ox-LDL).

showed thick fibrous cap with very weak to moderate yellow staining for collagen (score of 1-3), minimal to weak blue stain for glycans (score of 0-2), weak to moderate red stain for fibrin (score of 2-3), and minimal to very weak purple stain for elastin (score of 0-1) in the intima and media. The angioplasty + LPS group (Figure 4 panels E and E') revealed very weak to weak yellow staining for collagen (score of 1-2), minimal to weak blue stain for glycans (a score of 0-2), minimal to weak red stain for fibrin (score of 0-2), and minimal to strong purple stain for elastin (a score of 0-4). An elastin stain in the angioplasty + LPS group was present in the atherosclerotic plaque lesion as well as in the intima and media. The staining intensity for elastin was more in the media compared to the plaque lesion and nearly half the artery was stained for elastin in all swine. The angioplasty + oxLDL group (Figure 4 panels F and F') revealed minimal to very weak yellow stain for collagen (a score of 0-1), minimal to weak blue stain for glycans (a score of 0-2), very weak to weak red stain for fibrin (a score of 1-2), and minimal to weak purple stain for elastin (a score of 0-2). Elastin stain in the angioplasty + oxLDL group was present in the intima and media. All APA arteries in oxLDL-treated swine showed constricted lumen and a purple stain of the internal elastic lamina with medial hypertrophy. The collagen deposition on

the intimal surface of both oxLDL and LPS-treated arteries was comparable. Increased fibrin deposition of fibrin on the intimal surface of the oxLDL-treated arteries compared to LPS-treated arteries is again suggestive of an early stage of plaque formation. However, since these tissues were harvested 5-6 months after the initial intervention, there may be multiple time points where fresh lesions develop. Overall, the elastin and collagen stains were more in angioplasty with LPS and oxLDL group compared to angioplasty alone group (Table S2). Movat-Pentachrome staining of carotid arteries in the control, oxLDL, and LPS only groups without angioplasty revealed normal staining and morphology (Figure 2 panels B and D).

**Immunohistochemistry (IHC) showed increased immunopositivity for TLR-4 and TREM-1 in angioplasty with the oxLDL group:**

IHC for TLR-4 and TREM-1 in carotid arteries at the site of intervention revealed increased immunopositivity for TLR-4 and TREM-1 in the angioplasty + LPS and angioplasty + oxLDL group compared to angioplasty alone group (Figure 5). The positively stained cell density/mm<sup>2</sup> for TLR-4 was significantly higher in the angioplasty + oxLDL group compared to the angioplasty alone (244.55 ± 64.15

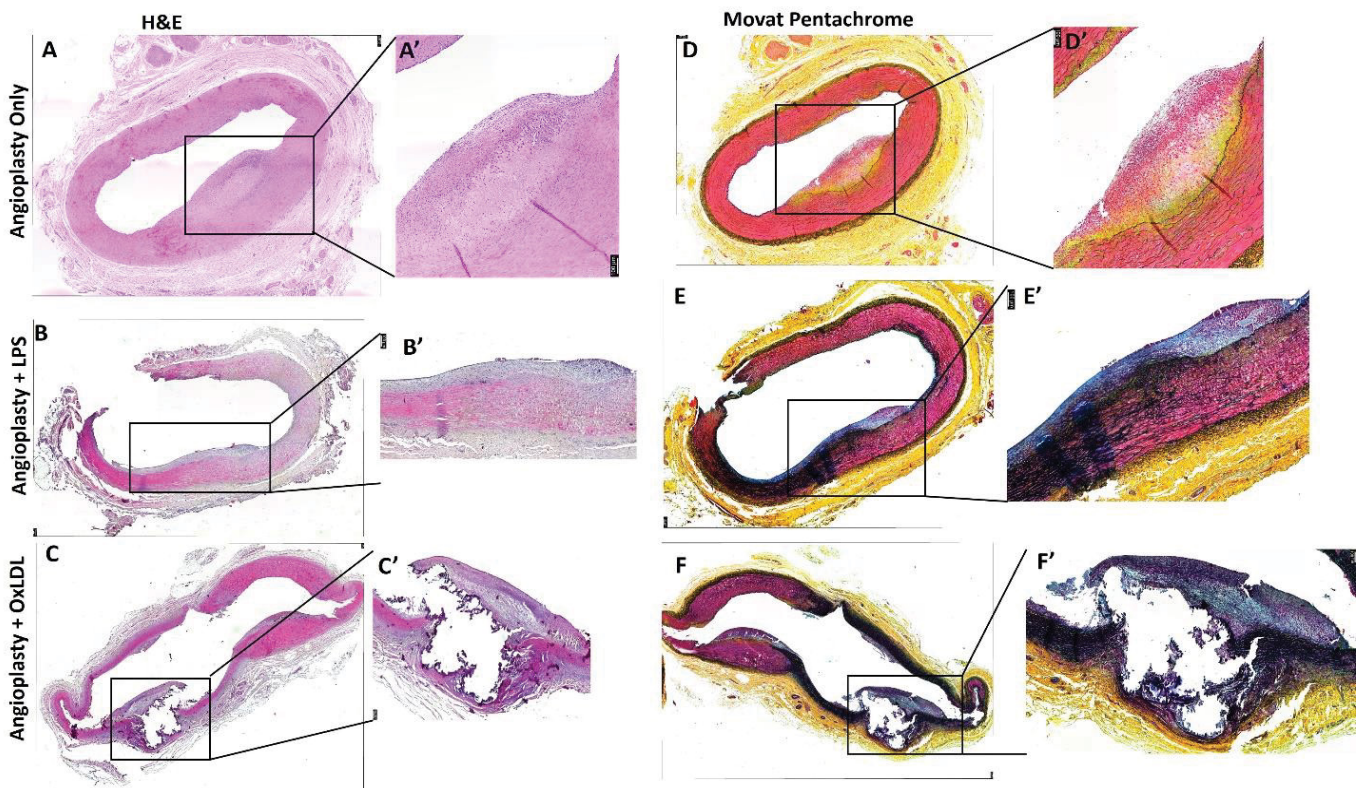


**Figure 3:** Hematoxylin and Movat-Pentachrome staining of carotid artery junction at the point of intervention. H & E staining of carotid artery junction at the site of intervention in angioplasty alone (panels A), angioplasty with LPS (panel B), and angioplasty with oxLDL (panel C); Movat-Pentachrome staining of carotid artery junction at the site of intervention in angioplasty alone (panels D), angioplasty with LPS (panel E), and angioplasty with oxLDL (panel F); panel A', B', C', D', E', and F' are the higher magnification images of the corresponding panels. All the images were scanned with 20X objective at a scale of 100µm while tile images were scanned at 50µm or 100µm.

vs  $36.70 \pm 21.00$ ;  $p=0.00156$ ) and angioplasty + LPS group ( $244.55 \pm 64.15$  vs  $27.80 \pm 8.27$ ;  $p=0.00438$ ) (Figure 5). Similarly, the positively stained cell density/mm<sup>2</sup> for TREM-1 was significantly higher in the angioplasty + oxLDL group compared to the angioplasty alone ( $415.90 \pm 68.91$  vs  $31.69 \pm 8.82$ ;  $p<0.0001$ ) and angioplasty + LPS group ( $415.90 \pm 68.91$  vs  $25.71 \pm 7.13$ ;  $p=0.00062$ ) (Figure 5).

IHC of the carotid arteries from all three groups showed immunopositivity for macrophages (CD14). The CD14 positively stained cell density/mm<sup>2</sup> was significantly increased in the angioplasty + oxLDL group compared to angioplasty alone ( $258.81 \pm 52.54$  vs  $15.40 \pm 8.87$ ;  $p<0.0001$ ) and angioplasty + LPS ( $258.81 \pm 52.54$  vs  $13.40 \pm 6.96$ ;  $p<0.0001$ ) group (Figure 5). The carotid arteries at the site of intervention showed immunopositivity for M1 macrophages (CD86) and M2 macrophages (CD206) in all three groups but there were no statistically significant differences between the groups (Figure 5). IHC of the carotid arteries at the site of intervention revealed immunopositivity with varied intensity for plaque instability markers including CD36 receptor or TSP-1, IL-12/23, MMP-7, and VCAM-1 in all three groups (Figure 6). The positively stained cell density/mm<sup>2</sup> for TSP-1 was significantly higher in angioplasty + the oxLDL group compared to angioplasty alone ( $42.22 \pm 11.25$  vs  $14.11 \pm$

$7.54$ ;  $p=0.0228$ ) and higher but not significant compared to angioplasty + LPS ( $42.22 \pm 11.25$  vs  $13.35 \pm 4.17$ ;  $p=0.0651$ ) group. Further, the positively stained cell density/mm<sup>2</sup> for IL-23 was significantly higher in the angioplasty + oxLDL group compared to angioplasty alone ( $45.13 \pm 14.62$  vs  $7.05 \pm 3.97$ ;  $p=0.0121$ ) and angioplasty + LPS ( $45.13 \pm 14.62$  vs  $15.44 \pm 10.26$ ;  $p=0.0087$ ) group (Figure 6). There was no significance for positively stained cell density for MMP-7 and VCAM-1 in between the three groups. Overall, a significantly increased number of CD14+, TREM-1+, TLR-4+, TSP-1+, IL-12/IL-23+ stained cells in the oxLDL group compared to LPS treated and angioplasty alone group, however, there was no trend in average stained intensity between the groups. This might be due to different plaque areas in different samples in each group or due to a limited number of animals in each group.

**Oxidized LDL significantly increased the mRNA expression of mediators of inflammation and plaque vulnerability:**

Real-time polymerase chain reaction (RT-PCR) results of the VSMCs and ECs isolated from Yucatan microswine carotid arteries and treated with either oxLDL or LPS for 24 hours showed significantly increased mRNA expression of mediators of inflammation. The mRNA expression of

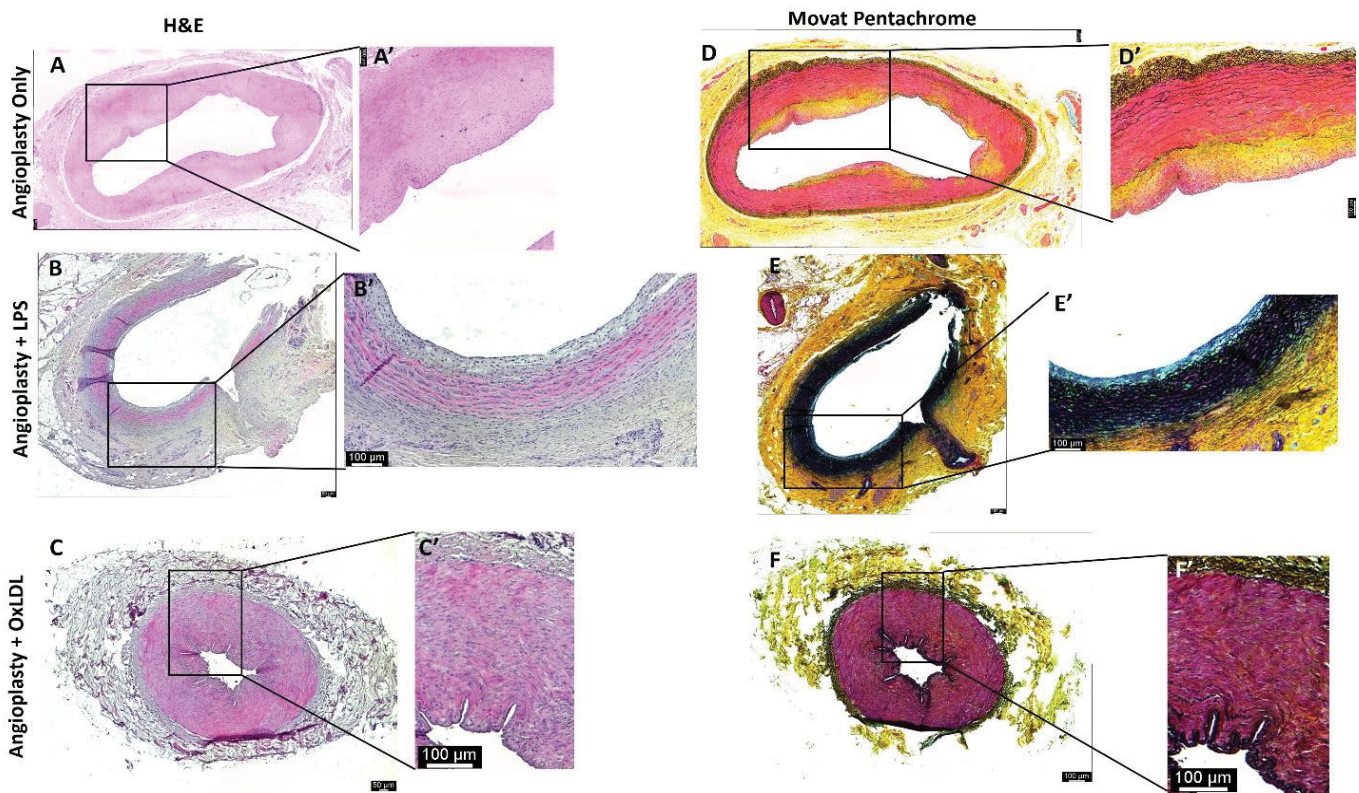


**Figure 4:** Hematoxylin and Movat-Pentachrome staining of the ascending pharyngeal artery at the point of intervention. H & E staining of the internal carotid artery at the site of intervention in angioplasty alone (panels A), angioplasty with LPS (panel B), and angioplasty with oxLDL (panel C); Movat-Pentachrome staining of the internal carotid artery at the site of intervention in angioplasty alone (panels D), angioplasty with LPS (panel E), and angioplasty with oxLDL (panel F); panel A', B', C', D', E', and F' are the higher magnification images of the corresponding panels. All the images were scanned with 20X objective at a scale of 100μm while tile images were scanned at 50μm or 100 μm.

mediators of inflammation including TREM-1, TLR-4, RelA, IKB, TIRAP, TRAM, TRIF, IL-6, and TNF- $\alpha$  and mediators regulating plaque vulnerability including collagen-I- $\alpha$ 1, collagen-III- $\alpha$ 1, vimentin, TSP-1, MMP-7, and VCAM-1 in VSMCs (Figure 7 panels A and C) and mRNA expression of collagen-I- $\alpha$ 1, TSP-1, MMP-7, RelA, IKB, TIRAP, TRAM, TRAF6, IL-6, TNF- $\alpha$ , VCAM-1, and TGF- $\beta$  in ECs was significantly increased with ox-LDL treatment (Figure 7 panels B and D). The mRNA expression of TREM-1, MyD88, collagen-I- $\alpha$ 1, collagen-III- $\alpha$ 1, vimentin, MMP-7, RelA, IKB, TIRAP, TRIF, TRAM, TRAF6, IL-6, TNF- $\alpha$ , VCAM-1, and TGF- $\beta$  in VSMCs (Figure 7 panels A and C) and the mRNA expression of TREM-1, TLR-4, MyD88, collagen-III- $\alpha$ 1, vimentin, RelA, TIRAP, TRAM, TRAF6, IL-6, TNF- $\alpha$ , VCAM-1, and TGF- $\beta$  in ECs were significantly increased with LPS treatment (Figure 7 panels B and D). It should be noted that the effect of oxLDL in increasing the expression of TLR-4 signaling was more prominent with oxLDL compared to LPS in VSMC. Collectively, PCR results revealed that oxLDL and LPS indeed affect the physiology of primary VSMCs and ECs, isolated from the carotid arteries

of swine and oxLDL has a more pronounced effect on the mRNA expression compared to LPS in VSMCs compared to ECs. Additionally, oxLDL is more potent compared to LPS in significantly increasing the mRNA expression of inflammatory mediators IL-6 and TNF- $\alpha$ , of TGF- $\beta$ , a mediator regulating myofibroblast reprogramming, and of VCAM-1, a marker for plaque vulnerability (Figure 7).

**ox-LDL is more potent than LPS in increasing protein expression of TLR-4, TIRAP, MMP-7, vimentin, and TSP-1:**

The Western Blot analysis results revealed that oxLDL significantly increased the protein expression of TLR-4, TIRAP, MMP-7, and TSP-1 compared to the control while an increase in the protein expression of TIRAP, vimentin, and TSP-1 was significantly increased with LPS compared to control. The protein expression of TLR-4, MMP-7, and TSP-1 was significantly increased with oxLDL compared to LPS (Figure 2 panel E). These results support that ox-LDL is more potent than LPS, albeit with differential potency for each protein marker of inflammation and plaque vulnerability.

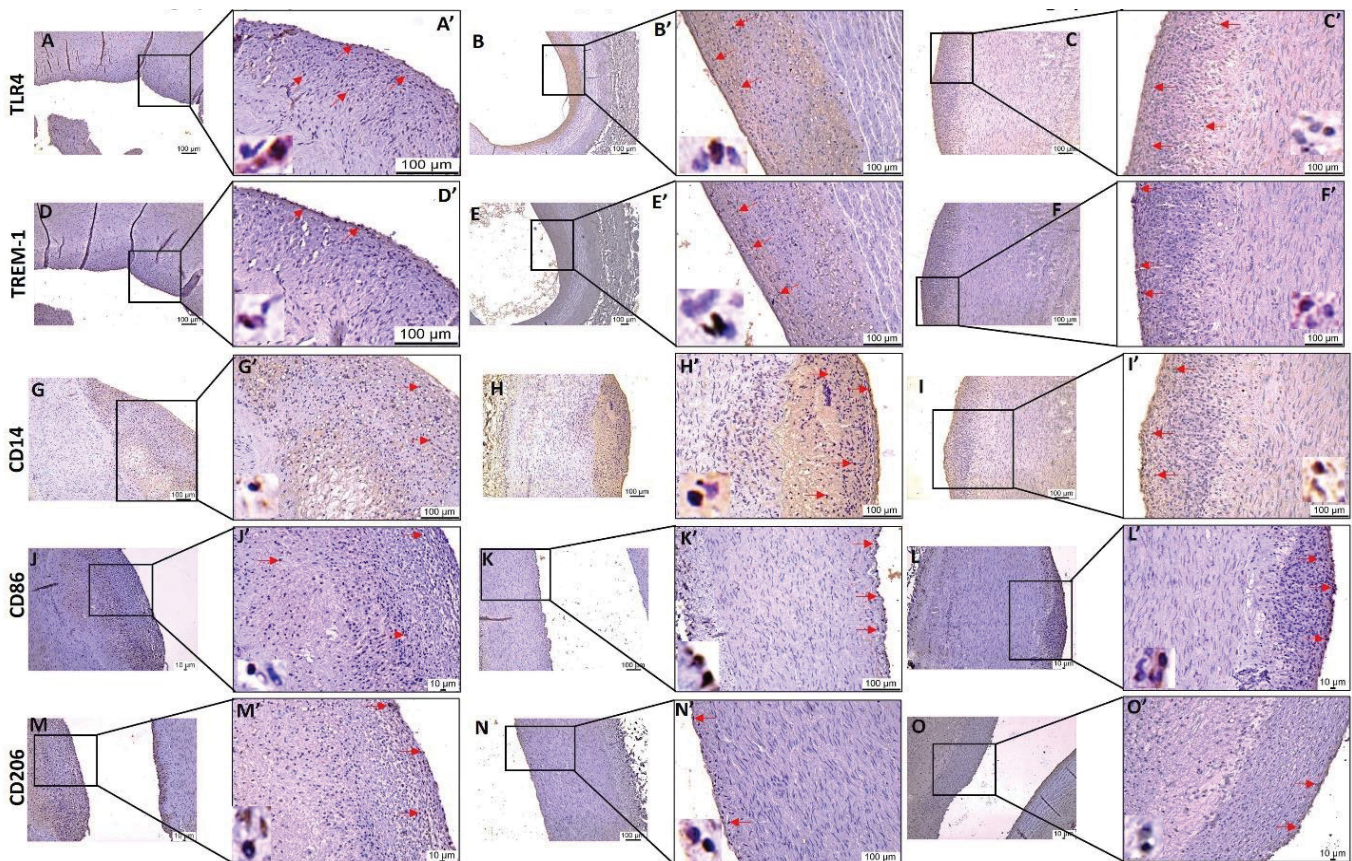


**Figure 5:** Immunohistochemistry for TLR4, TREM-1, CD14, CD86, and CD206 in carotid arteries. Immunostaining for TLR4 (panels A, B and C), TREM-1 (panels D, E and F), CD14 (panels G, H, and I), CD86 (panels J, K, and L), and CD206 (panels M, N, and O) in angioplasty alone, angioplasty with LPS and angioplasty with oxLDL respectively. Panels A', B', C'.... upto O' are corresponding images at higher magnification. The red arrows show the positively stained cells. Toll-like receptor (TLR)-4, triggering receptor expressed on myeloid cell (TREM)-1, lipopolysaccharide (LPS), and oxidized low-density lipoprotein (oxLDL). All the images were scanned with 20X objective at a scale of 100 $\mu$ m while tile images were scanned at 50 $\mu$ m or 100 $\mu$ m.

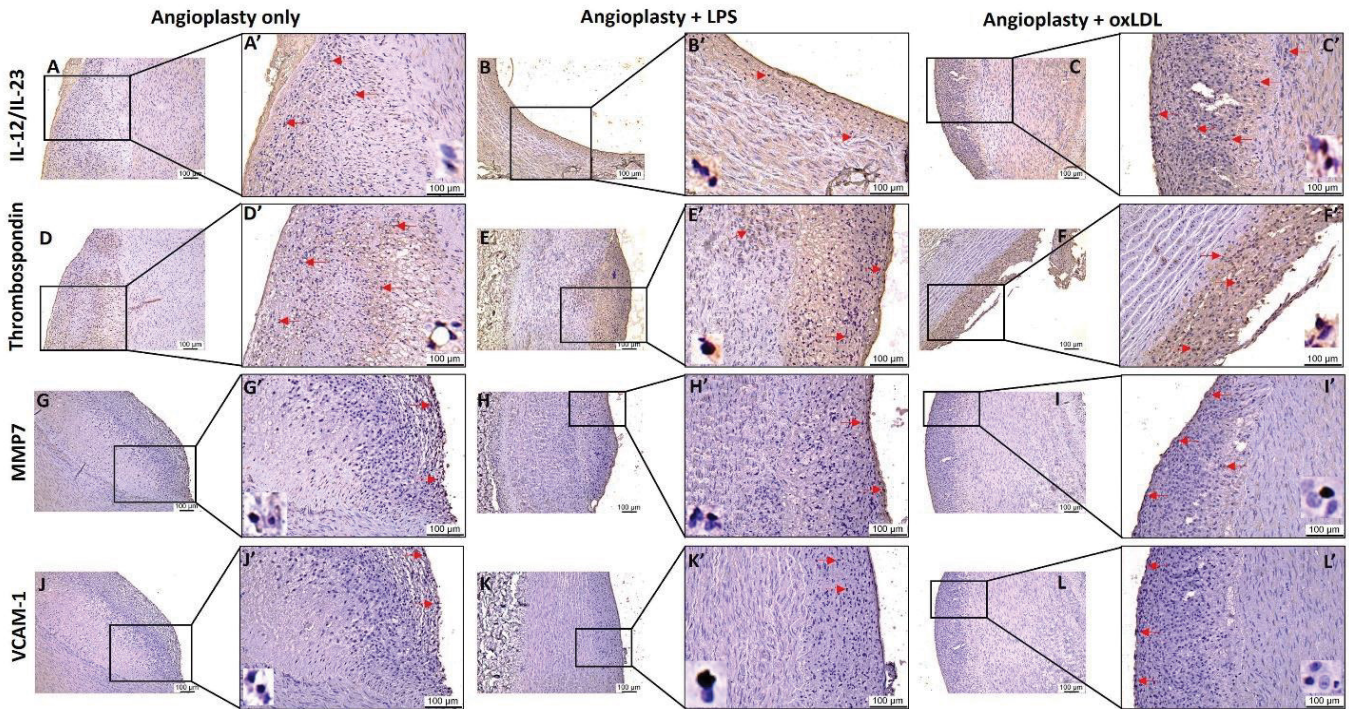


**Figure 6:** Immunohistochemistry for plaque instability markers IL-12/IL-23, thrombospondin (CD36 receptor), MMP7, and VCAM-1 in carotid arteries. Immunohistochemistry for interleukin (IL)-23 (panels A, B, and C), thrombospondin -1 (panels D, E, and F), matrix metalloproteinases (MMP)-7 (panels G, H, and I), and vascular cell adhesion molecule (VCAM)-1 (panels J, K, and L) in angioplasty alone, angioplasty with LPS, and angioplasty with oxLDL group. Panels A', B', C', D', E', F', G', H', I', J', K', and L' are higher magnification images for their corresponding image. Lipopolysaccharide (LPS), and minimally oxidized low-density lipoprotein (oxLDL). All the images were scanned with 20X objective at a scale of 100μm while tile images were scanned at 50μm or 100 μm.

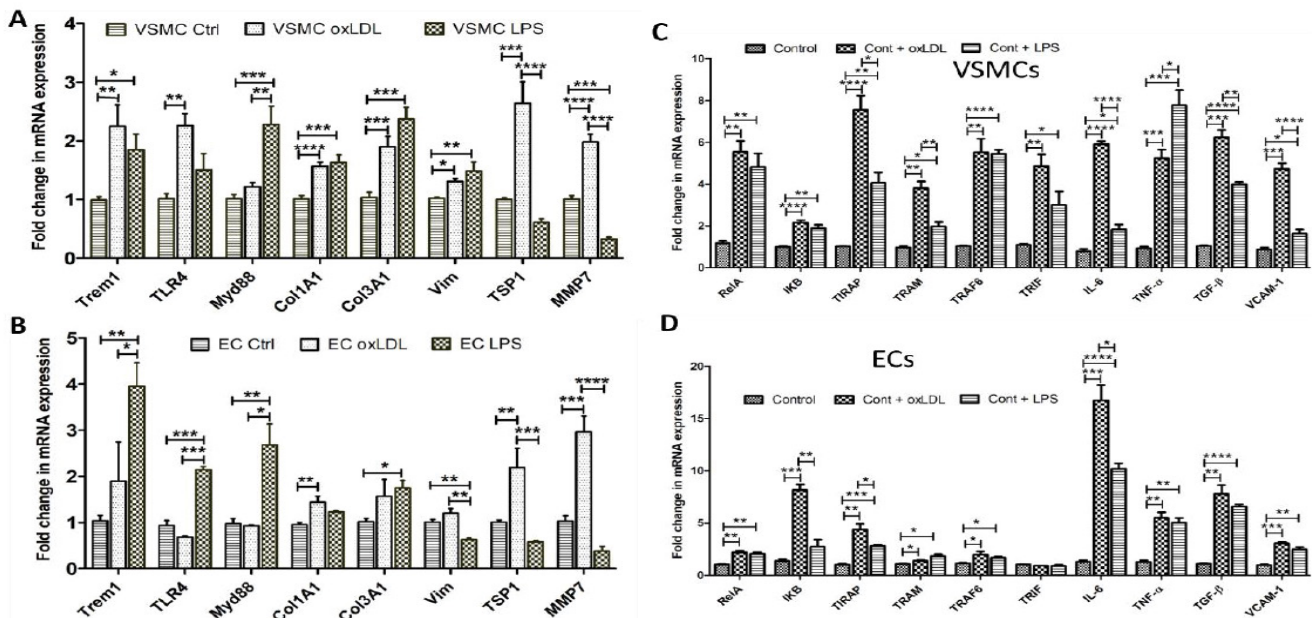


**Figure 7:** RT-PCR data showing fold change in the mRNA expression of the genes, triggering receptor expressed on myeloid cell (TREM), Toll-like receptor-4 (TLR-4), Myeloid differentiation primary response protein (Myd88), collagen-I-α1 (Col1A1), collagen-III-α1 (Col3A1), vimentin (Vim), Thrombospondin-1 (TSP-1), matrix metalloproteinase-7 (MMP-7), RelA (nuclear factor NF-kappa-B p65 subunit), IKK, TRAP (Toll-interleukin-1 Receptor (TIR) domain-containing adaptor protein), TRAM (TRIF-related adaptor molecule), TRAF6 (TNF receptor associated factor 6), TRIF (TIR-domain-containing adapter-inducing interferon-β), interleukin (IL)-6, tumor necrosis factor (TNF)-α, transforming growth factor (TGF)-β, and VCAM (vascular cell adhesion protein)-1 in primary vascular smooth muscle cells (panels A and C) and in primary vascular endothelial cells (panels B and D) treated with lipopolysaccharide (LPS), and oxidized low-density lipoprotein (oxLDL). \*p < 0.05, \*\*p < 0.01, \*\*\*p < 0.001 and \*\*\*\*p < 0.0001.

## Discussion

Atherosclerosis is initiated by the homing and oxidation of LDL particles in the subintimal space due to the entrapment by high-affinity glycoproteins present in the intimal matrix [37]. Ox-LDL triggers a cascade of pro-inflammatory events including foam cell formation, neointimal hyperplasia, and eventually plaque formation [38]. Importantly, hypercholesterolemia and turbulent blood flow result in increased susceptibility of the vessel segments with low wall shear stress for plaque formation [37]. Hence, the loss of intimal integrity and ox-LDL burden mark the crucial biological events in atheroma formation. The biological mechanisms underlying oxLDL-induced pro-atherogenic lesions in translationally worthwhile large animal models are few in the literature. We have developed the Yucatan microswine model of unstable carotid plaque formation which closely resembles the human carotid plaque by a combination of high cholesterol diet and balloon angioplasty. This model also allows us to deliver agents such as LPS and oxLDL that can induce vulnerable plaques directly at the site of intimal injury which increases the site-specific bioavailability and bioretention in the subintimal space. To the best of our knowledge, we are the first to induce robust atherosclerotic lesions over a period of 1 year in Yucatan microswine which have been fed a high-fat diet for 4-5 months, performed angioplasty surgeries with local delivery of ox-LDL or LPS and then followed up for another 5-6 months to best simulate human atherosclerotic lesions. In the present study, we used high-resolution ultrasound to evaluate IMT in the common carotid artery [39]. Despite the expected variability between pigs, increased IMT in the angioplasty + ox-LDL in contrast to the angioplasty + LPS and angioplasty alone control groups on US imaging suggest that ox-LDL is relatively more robust than to LPS after intimal injury. LPS has been used as an exogenous inducer of atherosclerosis in multiple animal models which exhibited promising findings [26]. However, the endogenous nature, biochemical and clinical significance, and active involvement in sterile inflammation favor ox-LDL to be the ideal choice for translationally relevant pre-clinical models in atherosclerosis. A 36% increase in common carotid IMT (a surrogate marker for atherosclerosis) in angioplasty + oxLDL swine advocates the pathological impact of ox-LDL in our study which was further supported by OCT and immuno/histology findings. We performed US imaging of the common carotid artery only, as APA was not accessible by US in Yucatan microswine. To scan the APA for the presence of atherosclerotic plaque, we used angiography and OCT. The angiography of the common carotid and APA were inconclusive due to the lower degree of stenosis and the small size of the plaque which cannot be detected by angiography. Angiography can only detect carotid diameter stenosis that is greater than 50% [40]. The presence of mixed-signal rich and signal-poor concentric and eccentric plaques with poor visualization of the three layers of the artery in the

angioplasty alone group and the features of larger stable and unstable plaques in the LPS and ox-LDL groups suggest the potency of LPS and ox-LDL in inducing plaque formation and progression after intimal injury [21, 41] (Figure 1). Among the LPS and ox-LDL groups, ox-LDL treatment induces features of plaque instability more than LPS. This may be due to injected minimally ox-LDL and continued oxidation of LDL in the plaque transported from plasma. LPS also enhances plaque vulnerability by promoting lipid accumulation [21, 41]. The signs of necrotic core, intraplaque hemorrhage, and ruptured plaque in the oxLDL-treated group mainly at the carotid junction on OCT suggest oxLDL to be more potent than LPS (Figure 1). The potency of ox-LDL and LPS after intimal injury in inducing plaque is further supported by the results that alone ox-LDL or LPS without angioplasty does not induce plaque formation (Figure 2). This also suggests that endothelial dysfunction and increased permeability initiate plaque formation [42] and the presence of hypercholesterolemia or inflammation adds to it and precipitate plaque vulnerability and rupture with time.

Increased plaque size, presence of chronic inflammation, necrotic core, and ruptured plaques in the oxLDL group compared to LPS and angioplasty alone group on H & E and increased elastin degradation and collagen stain on Movat Pentachrome staining [4-6, 43] further support the OCT and US findings and the potency of oxLDL and LPS in inducing plaque vulnerability with a predominant effect of ox-LDL [21,41] (Figures 1, 3, and 4). Interestingly, the narrowed lumen of APA in the oxLDL group (Figure 4) might be caused largely by reactive hyperplasia and arterial remodeling in response to intimal injury during intervention [44] and due to the replacement of the granulation tissue by scar and a variable extent of fibrosis and remodeling with time [45] as revealed on Movat-pentachrome staining (Yucatan microswine was reassessed after 5-6 months of intervention). Increased elastin and collagen expression in oxLDL-treated arteries are supported by the fact that during atherosclerosis, elastin degradation occurs but the synthesis of tropoelastin increases, and this is compensated by increased collagen which is stiffer than elastin [46]. LPS increases elastin production through fibroblasts in atherosclerosis and an increased accumulation of LDL. Increased staining for collagen and elastin in this study in LPS and oxLDL-treated arteries suggest increased tropoelastin or lipid accumulation (due to injected oxLDL) in the arteries, which is the underlying etiology for atherosclerosis [46] (Figures 2 and 4, and Table S2). Furthermore, increased fibrin deposition and alteration in glycan structure play a crucial role in the pathogenesis of atherosclerosis [47] and increased staining for fibrin and glycan in LPS and oxLDL treated arteries compared to angioplasty alone group suggests the role of LPS and oxLDL in increasing fibrin and glycans content in atherosclerosis (Figures 3 and 4, Table S2). However, the underlying mechanisms warrant further investigation at

earlier time points after the intervention. Collectively, the results from ultrasound, OCT, H&E, and Movat-Pentachrome staining support the notion that LPS and oxLDL induce plaque formation and vulnerability after intimal injury with more pronounced effects with oxLDL.

Sterile inflammation plays a critical role in the progression of atherosclerosis and ox-LDL has been identified to be a potent DAMP molecule aggravating the pathology [48]. Activation and signaling through TREM1 and TLR4 are crucial events associated with sterile inflammation in atherosclerosis [8, 14-16, 49]. The pro-inflammatory niche in the atheroma due to the increased density of immune cells, especially the M1 macrophages [50] suggests macrophages as a major contributor to atherosclerosis. A significantly increased immunopositivity for CD14, CD86 (M1 macrophage), and CD206 (M2 macrophages) in all three groups suggests chronic inflammation in plaque (Figure 5). Chronicity of inflammation is further supported by a significantly increased expression of TREM1 and TLR4 in the ox-LDL group compared to angioplasty with LPS and angioplasty alone group (Figure 5) and this may have contributed to increased plaque vulnerability in the oxLDL group [21,51]. Not only vessel stenosis but also plaque vulnerability should be considered for screening high-risk patients. Computed tomography, magnetic resonance imaging, US imaging, IMT measurement, molecular imaging, and blood LDL levels are commonly used diagnostics [52]. Plasma levels of C-reactive proteins, fibrinogen, leukocytes MMP-7, IL23, visfatin granzyme B, CD-36, IL-6, VCAM-1, TNF $\alpha$ , pentraxin 3, higher levels of MMP-1, MMP-2, MMP-7, MMP-8, MMP-12, and MMP-14, and others have been postulated to be associated with plaque vulnerability [22-26, 52-54]. However, there is no definitive marker(s) to screen and diagnose vulnerability. Increased fibrinogen, leukocytes MMP-7, IL23, visfatin granzyme B, CD-36, IL-6, and VCAM-1 are biomarkers of plaque vulnerability [52]. A positive staining for TREM-1, TLR-4, MMP-7, IL12/23, CD-36 (TSP-1), IL-6, TNF- $\alpha$ . and VCAM-1 in all three groups and a significantly higher expression of TSP-1 and IL-23 and similar levels of MMP-7 and VCAM-1 in the ox-LDL group compared to the angioplasty + LPS and angioplasty alone group (Figures 5 and 6) suggest more pronounced effects of ox-LDL on plaque vulnerability compared to LPS and angioplasty alone [22, 23]. These findings were further supported by the significantly increased mRNA expression of mediators of inflammation and plaque vulnerability in VSMCs and ECs treated with oxLDL and LPS (Figure 7). PCR studies revealing significantly increased mRNA expression of TSP-1 and MMP-7 with oxLDL but not with LPS in VSMCs and ECs (Figure 7) suggests greater atherogenic and vulnerability effects of oxLDL compared to LPS [42, 52]. However, decreased mRNA expression of TSP-1 and MMP-7 in ECs with LPS and of TLR-4 with oxLDL warrants investigation. One possibility might be the effects of the constituents of oxidized LDL used to treat the

ECs. Overall, significantly increased mRNA expression of plaque instability markers TSP-1 and MMP-7 with oxLDL compared to LPS suggest more pronounced effects of oxLDL on plaque vulnerability. These findings at the gene level were also supported by the Western Blot analysis where oxLDL is more potent in increasing the protein expression of TLR-4 and TIRAP (mediators of inflammation) and MMP-7 and TSP-1 (markers of plaque vulnerability) in VSMCs.

A significantly increased expression of TLR-4 and its downstream signaling, TREM-1, and mediators of plaque vulnerability in carotid arteries collected from ox-LDL and LPS treated swine and VSMCs and ECs isolated from Yucatan microswine carotid arteries suggest the atherogenic potential of ox-LDL and LPS after intimal injury with a more pronounced effect with oxLDL. This notion is supported by our previous findings that oxLDL compared to LPS is more potent in increasing S10012, another marker for plaque progression and vulnerability [55], and that inflammation regulates the phenotypic switch of VSMCs to different phenotypes including contractile, proliferative, and dedifferentiated subtypes [56] contributing to plaque formation and vulnerability. Since the proliferation, migration, and phenotypic switching of VSMCs play a critical role in plaque development and progression [57,58], targeting oxLDL- and LPS-induced inflammation could have therapeutic importance. Additionally, normal histomorphological and radiological findings in the arteries of the control, only LPS, and only oxLDL groups without angioplasty suggest that oxLDL and LPS induce inflammation and increase expression of other mediators involved in plaque progression but intimal injury [13, 59] is an inducing event and in conjunction with LPS and oxLDL adds to plaque burden. This is supported by the results from arteries undergoing angioplasty and then treated with LPS and ox-LDL in other experimental groups. Collectively, the results of this study support the potential of oxLDL and LPS in inducing plaque vulnerability with oxLDL being relatively more potent in inducing plaque development, progression, and vulnerability after intimal injury. Further, an increased expression of mediators of inflammation TLR-4 and TREM-1 in association with ox-LDL and LPS treatment suggests the cause-effect relationship of these factors in neointimal hyperplasia and plaque formation and vulnerability and targeting TLR-4 and TREM-1 as therapeutic targets. However, this relationship needs to be investigated further using transcriptomics and proteomics analysis to delineate a gene-protein, protein-protein, and causal network relationship. This notion is supported by the fact that not only genetic factors, but also epigenetic factors (transcription and transcriptional factors) play a role in neointimal hyperplasia, thrombosis, and stenosis [60-63]. Further, these analyses are also important because it is not only the vascular inflammation but also the perivascular inflammation that plays a role in neointimal hyperplasia and stenosis after intimal injury [64,65]. Furthermore, delineating a cause-effect relation between the infiltrating

immune cells and plaque formation and vulnerability along with the factors regulating these effects is also important. This is important because an altered immune response plays a critical role in atherosclerosis [66, 67]. Moreover, VSMC and ECs play a critical role in neointimal hyperplasia and plaque development and vulnerability, as supported by the data from this study, and the phenotypic changes in VSMC phenotype and function [56] with oxLDL and LPS treatment should be investigated using omics studies. The results of this study revealed that oxLDL and LPS increase TLR-4 expression and the findings that inhibiting TLR-4 attenuates NIH, stenosis, and thrombosis support the notion of targeting oxLDL-induced TLR-4 and TREM-1 to attenuate plaque vulnerability[33]. Above mentioned and other studies [68-72] suggest that transcriptomics and proteomics analysis of the tissues collected after oxLDL and LPS treatment will be informative and investigate newer perspectives and novel therapeutic targets to attenuate plaque progression and vulnerability.

### Limitations of the study

Despite the robust induction of atherosclerotic lesions in Yucatan microswine, our study was not without limitations. Firstly, we could have used more swine in each experimental group due to some variability between the animals even in the same batch. However, the enormous cost of acquiring and maintaining the swine for many months prohibited us to do so. Hence, we are cautious in interpreting and concluding that ox-LDL is better than LPS. Secondly, we are not sure about the optimal amount of oxLDL vs LPS that needs to be used to conclusively say which of these is more potent. We used moderately pure oxLDL which was partially oxidized with copper sulfate to 2µM as measured by TBARs assay which is equivalent to about 40 nanomoles of MDA per mg of protein. This assay does not distinguish between minimally modified vs oxidized LDL[73] where only the lipids are oxidized in minimally modified LDL and both lipids and proteins are oxidized in ox-LDL prepared with copper sulfate. Hence, there could be a variation in the amount of oxidized lipid, which is the main pathogenetic component of ox-LDL, that was delivered and absorbed into the intimal lesions. Thirdly, even though we blocked the arterial flow at the proximal part of the carotid artery near the site of intervention, some blood might still flow in reverse into the site of intervention and wash off the injected oxLDL and LPS to varying degrees which we cannot measure. Fourthly, numerous longitudinal imaging studies in humans have demonstrated that plaque morphology can change over just a few months while gaining or losing the characteristics of vulnerability[74,75]. Since our study spanned for up to six months after the initial intervention where the swine were continued on a high-cholesterol diet, it is possible that the lesions might be evolving into vulnerable or stable and extending longitudinally into areas not part of the site of intervention. In fact, our OCT study in some

animals found lesions beyond the site of intervention which we have not studied by histology. Lastly, it is well known that the inflammatory status of an individual can significantly contribute to acute vascular events as evidenced by large phase 3 trials of the anti-inflammatory agent's paramount in causing major cardiovascular events[11,76,77]. Another limitation is that atherosclerosis in this model was induced after injury with balloon angioplasty and therefore is less representative of natural atherosclerosis seen in humans. Human atherosclerosis happens in intact endothelium as a "response to LDL" and not in mechanically injured endothelium ("response to injury"). Additionally, the APA tissue collected for histology was mostly fibrosed at the site of intervention and only one artery had clear histology. In the remaining samples, the artery near the site of intervention was used and it showed constricted lumen and thinned walls. Based on these findings, it is essential to do future studies with a greater number of animals and check more APA at the site of intervention. Despite our swine being housed in specific pathogen-free facilities, we did observe skin and digestive tract infections which could have altered the inflammatory status leading to the worsening of some swine and not others. This further suggests the need for omics studies to investigate epigenetic aspects. Nonetheless, with all the above limitations, the current study established a translationally worthwhile pre-clinical model closely simulating the human carotid artery atherosclerosis which would open novel opportunities in atherosclerosis research.

### Conclusion

The incidence of atherosclerotic plaque rupture increases with age, however, the underlying molecular mechanisms and the factors inducing plaque vulnerability are still ambiguous. Inflammation and hypercholesterolemia play a crucial role in the pathogenesis of atherosclerosis and plaque vulnerability. In this study, we investigated the effect of direct infusion of LPS and oxLDL on inducing plaque formation and plaque vulnerability. The results revealed increased incidences of plaque vulnerability with LPS and oxLDL with more pronounced effects with oxLDL. A significantly increased expression of TREM-1, TLR-4, macrophages, and markers of plaque vulnerability TSP-1 and IL-23 suggested the potency of oxLDL in inducing inflammation and plaque vulnerability and TLR-4 and TREM-1 as potential therapeutic targets. Further studies with an increased number of swine treated with ox-LDL injected after angioplasty are warranted to unravel the underlying mechanisms, types of immune and vascular cells involved, and the regulatory signaling associated with ox-LDL mediated plaque vulnerability and the potency of ox-LDL in inducing plaque vulnerability..

### Authors' contributions:

Concept and design: VR, MMR, DKA; Tissue collection: SN, VR, MMR, FGT, HS; Acquisition of data: SN, VR, HS,

and MMR; Analysis and interpretation of data: SN, VR, MMR; Drafting the article: SN and VR; Revising and editing the manuscript: MMR, HS, FGT, YSC, DKA; Final approval of the article: SN, VR, MMR, FGT, HS, YSC, DKA.

### Funding:

This work was supported by the research grants R01 HL144125 and R01HL147662 to DKA from the National Heart, Lung, and Blood Institute, National Institutes of Health, USA. The contents of this chapter are solely the responsibility of the authors and do not necessarily represent the official views of the National Institutes of Health.

### Institutional review board statement:

Not applicable. All institutional and national guidelines for the care and use of laboratory animals were followed and approved by the appropriate institutional committees (Protocols #1017 and #R191ACUC026).

### Informed consent statement:

Not applicable.

### Data availability statement:

All the analyzed data have been provided in the manuscript and Supplementary Files. The datasets (raw data) used for analysis during the current study will be made available by the corresponding author upon request.

### Conflicts of interest:

The authors declare no conflict of interest..

### References

1. Virani SS, Alonso A, Aparicio HJ, et al. Heart disease and stroke statistics-2021 update: a report from the american heart association. *Circulation* 143 (2021): 254-743.
2. Narula J, Nakano M, Virmani R, et al. Histopathologic characteristics of atherosclerotic coronary disease and implications of the findings for the invasive and noninvasive detection of vulnerable plaques. *J Am Coll Cardiol* 61 (2013): 1041-1051.
3. Kaul S, Narula J. In search of the vulnerable plaque: is there any light at the end of the catheter? *J Am Coll Cardiol* 64 (2014): 2519-2524.
4. Kolodgie FD, Virmani R, Burke AP, et al. Pathologic assessment of the vulnerable human coronary plaque. *Heart* 90 (2004): 1385-1391.
5. Shi ZS, Feng L, He X, et al. Vulnerable plaque in a Swine model of carotid atherosclerosis. *AJNR Am J Neuroradiol* 30 (2009): 469-472.
6. Newby AC. Metalloproteinases and vulnerable atherosclerotic plaques. *Trends Cardiovasc Med* 17 (2007): 253-258.
7. Libby P, Aikawa M. Stabilization of atherosclerotic plaques: new mechanisms and clinical targets. *Nat Med* 8 (2002): 1257-1262.
8. Rai V, Agrawal DK. The role of damage- and pathogen-associated molecular patterns in inflammation-mediated vulnerability of atherosclerotic plaques. *Can J Physiol Pharmacol* 95 (2017): 1245-1253.
9. Samuel M, Tardif JC. Lessons learned from large cardiovascular outcome trials targeting inflammation in cardiovascular disease (CANTOS, CIRT, COLCOT and LoDoCo2). *Future Cardiol* 17 (2021): 411-414.
10. Swerdlow DI, Holmes MV, Kuchenbaecker KB, et al. The interleukin-6 receptor as a target for prevention of coronary heart disease: a mendelian randomisation analysis. *Lancet* 379 (2012): 1214-1224
11. Ridker PM, Everett BM, Thuren T, et al. Antiinflammatory therapy with canakinumab for atherosclerotic disease. *N Engl J Med* 377 (2017): 1119-1131.
12. Mitra AK, Dhume AS, Agrawal DK. "Vulnerable plaques"--ticking of the time bomb. *Can J Physiol Pharmacol* 82 (2004): 860-8671.
13. Rai V, Agrawal DK. Renin angiotensin system in the maturation and failure of arterio-venous fistula. *The Renin Angiotensin System in Cardiovascular Disease: Springer* (2023): 291-303.
14. Rai V, Rao VH, Shao Z, Agrawal DK. Dendritic cells expressing triggering receptor expressed on myeloid cells-1 correlate with plaque stability in symptomatic and asymptomatic patients with carotid stenosis. *Plos one* 11 (2016): 0154802.
15. Rao VH, Rai V, Stoupa S, Subramanian S, et al. Data on TREM-1 activation destabilizing carotid plaques. *Data Brief* 8 (2016): 230-234.
16. Rao VH, Rai V, Stoupa S, et al. Tumor necrosis factor-alpha regulates triggering receptor expressed on myeloid cells-1-dependent matrix metalloproteinases in the carotid plaques of symptomatic patients with carotid stenosis. *Atherosclerosis* 248 (2016): 160-169.
17. Fuster JJ. TLR4 in Atherogenesis: Paying the Toll for Antimicrobial Defense. *J Am Coll Cardiol* 71 (2018): 1571-1573.
18. Brown MS, Goldstein JL. Lipoprotein metabolism in the macrophage: implications for cholesterol deposition in atherosclerosis. *Annu Rev Biochem* 52 (1983): 223-261.
19. Kostner GM. Lipoprotein receptors and atherosclerosis. *Biochem Soc Trans* 17 (1989): 639-641.
20. Obermayer G, Afonyushkin T, Binder CJ. Oxidized low-density lipoprotein in inflammation-driven thrombosis. *J Thromb Haemost* 16 (2018): 418-428.

21. Nishi K, Itabe H, Uno M, et al. Oxidized LDL in carotid plaques and plasma associates with plaque instability. *Arterioscler Thromb Vasc Biol* 22 (2002): 1649-1654.
22. Stenina OI, Plow EF. Counterbalancing forces: what is thrombospondin-1 doing in atherosclerotic lesions? *Circ Res* 103 (2008): 1053-1055.
23. Abbas A, Gregersen I, Holm S, et al. Interleukin 23 levels are increased in carotid atherosclerosis: possible role for the interleukin 23/interleukin 17 axis. *Stroke* 46 (2015): 793-799.
24. Olejarz W, Lacheta D, Kubiak-Tomaszewska G. Matrix metalloproteinases as biomarkers of atherosclerotic plaque instability. *Int J Mol Sci* 21 (2020): 3946.
25. Weinkauff CC, Concha-Moore K, Lindner JR, et al. Endothelial vascular cell adhesion molecule 1 is a marker for high-risk carotid plaques and target for ultrasound molecular imaging. *J Vasc Surg* 68 (2018): 105-113.
26. Bowman JD, Surani S, Horseman MA. Endotoxin, toll-like receptor-4, and atherosclerotic heart disease. *Curr Cardiol Rev* 13 (2017): 86-93.
27. Lee YT, Lin HY, Chan YW, et al. Mouse models of atherosclerosis: a historical perspective and recent advances. *Lipids Health Dis* 16 (2017): 12.
28. Bashir AZ, Bashir K, Hunter WJ, et al. Cathepsin L expression in the carotid arteries of atherosclerotic swine. *Arch Med Sci Atheroscler Dis* 4 (2019): 264-267.
29. Dhume AS, Soundararajan K, Hunter WJ, et al. Comparison of vascular smooth muscle cell apoptosis and fibrous cap morphology in symptomatic and asymptomatic carotid artery disease. *Ann Vasc Surg* 17 (2003): 1-8.
30. van Koevorden ID, de Bakker M, Haitjema S, et al. Testosterone to oestradiol ratio reflects systemic and plaque inflammation and predicts future cardiovascular events in men with severe atherosclerosis. *Cardiovasc Res* 115 (2019): 453-462.
31. Carroll JA, Carter DB, Korte SW, et al. Evaluation of the acute phase response in cloned pigs following a lipopolysaccharide challenge. *Domest Anim Endocrinol* 29 (2005): 564-572.
32. Ogita M, Miyauchi K, Onishi A, et al. Development of accelerated coronary atherosclerosis model using low density lipoprotein receptor knock-out swine with balloon injury. *Plos one* 11 (2016): 0163055.
33. Rai V, Radwan MM, Nooti S, et al. TLR-4 Inhibition attenuates inflammation, thrombosis, and stenosis in arteriovenous fistula in yucatan miniswine. *Cardiol Cardiovasc Med* 6 (2022): 432-450.
34. Li K, Wong DK, Luk FS, et al. Isolation of plasma lipoproteins as a source of extracellular RNA. *Methods Mol Biol* 1740 (2018): 139-153.
35. Randrianarisoa E, Rietig R, Jacob S, et al. Normal values for intima-media thickness of the common carotid artery--an update following a novel risk factor profiling. *Vasa* 44 (2015): 444-450.
36. Paul J, Shaw K, Dasgupta S, et al. Measurement of intima media thickness of carotid artery by B-mode ultrasound in healthy people of India and Bangladesh, and relation of age and sex with carotid artery intima media thickness: An observational study. *J Cardiovasc Dis Res* 3 (2012): 128-131.
37. Mughal MM, Khan MK, DeMarco JK, et al. Symptomatic and asymptomatic carotid artery plaque. *Expert Rev Cardiovasc Ther* 9 (2011): 1315-1330.
38. Lara-Guzman OJ, Gil-Izquierdo A, Medina S, et al. Oxidized LDL triggers changes in oxidative stress and inflammatory biomarkers in human macrophages. *Redox Biol* 15 (2018): 1-11.
39. Steinel DC, Kaufmann BA. Ultrasound imaging for risk assessment in atherosclerosis. *Int J Mol Sci* 16 (2015): 9749-9769.
40. Jiangping S, Zhe Z, Wei W, et al. Assessment of coronary artery stenosis by coronary angiography: a head-to-head comparison with pathological coronary artery anatomy. *Circ Cardiovasc Interv* 6 (2013): 262-268.
41. Wang J, Si Y, Wu C, et al. Lipopolysaccharide promotes lipid accumulation in human adventitial fibroblasts via TLR4-NF-kappaB pathway. *Lipids Health Dis* 11 (2012): 139.
42. Gimbrone MA, Jr., Garcia-Cardena G. Endothelial cell dysfunction and the pathobiology of atherosclerosis. *Circ Res* 118 (2016): 620-636.
43. Finn AV, Nakano M, Narula J, et al. Concept of vulnerable/unstable plaque. *Arterioscler Thromb Vasc Biol* 30 (2010): 1282-1292.
44. Geary RL, Nikkari ST, Wagner WD, et al. Wound healing: a paradigm for lumen narrowing after arterial reconstruction. *J Vasc Surg* 27 (1998): 96-106.
45. Martin P. Wound healing--aiming for perfect skin regeneration. *Science* 276 (1997): 75-81.
46. Coccione AJ, Hawes JZ, Staiculescu MC, et al. Elastin, arterial mechanics, and cardiovascular disease. *Am J Physiol Heart Circ Physiol* 315 (2018): 189-205.
47. Eckardt V, Weber C, von Hundelshausen P. Glycans and glycan-binding proteins in atherosclerosis. *Thromb Haemost* 119 (2019): 1265-1273.
48. Khwaja B, Thankam FG, Agrawal DK. Mitochondrial

- DAMPs and altered mitochondrial dynamics in OxLDL burden in atherosclerosis. *Mol Cell Biochem* 476 (2021): 1915-1928.
49. Kouassi KT, Gunasekar P, Agrawal DK, et al. TREM-1; Is It a Pivotal Target for Cardiovascular Diseases? *J Cardiovasc Dev Dis* 5 (2018): 45.
  50. Barrett TJ. Macrophages in atherosclerosis regression. *Arterioscler Thromb Vasc Biol* 40 (2020): 20-33.
  51. Rhoads JP, Major AS. How Oxidized Low-Density Lipoprotein Activates Inflammatory Responses. *Crit Rev Immunol* 38 (2018): 333-342.
  52. Skagen K, Skjelland M, Zamani M, et al. Unstable carotid artery plaque: new insights and controversies in diagnostics and treatment. *Croat Med J* 57 (2016): 311-320.
  53. Wang Y, Wang T, Luo Y, et al. Identification markers of carotid vulnerable plaques: An Update. *Biomolecules* 12 (2022): 1192
  54. Shindo A, Tanemura H, Yata K, et al. Inflammatory biomarkers in atherosclerosis: pentraxin 3 can become a novel marker of plaque vulnerability. *PLoS One* 9 (2014): 100045.
  55. Singh H, Rai V, Agrawal DK. LPS and oxLDL-induced S100A12 and RAGE expression in carotid arteries of atherosclerotic Yucatan microswine. *Mol Biol Rep* 49(2022): 8663-8672.
  56. Rai V, Singh H, Agrawal DK. Targeting the crosstalk of immune response and vascular smooth muscle cells phenotype switch for arteriovenous fistula maturation. *Int J Mol Sci* 23 (2022): 12012.
  57. Bennett MR, Sinha S, Owens GK. Vascular smooth muscle cells in atherosclerosis. *Circ Res* 118 (2016): 692-702.
  58. Pan J, Cai Y, Liu M, et al. Role of vascular smooth muscle cell phenotypic switching in plaque progression: A hybrid modeling study. *J Theor Biol* 526 (2021): 110794.
  59. Velpuri P, Rai V, Agrawal DK. Role of sirtuins in attenuating plaque vulnerability in atherosclerosis. *Molecular and Cellular Biochemistry* (2023):1-12.
  60. Singh D, Rai V, Agrawal DK. Non-Coding RNAs in regulating plaque progression and remodeling of extracellular matrix in atherosclerosis. *Int J Mol Sci* 23 (2022): 13731.
  61. Rai V, Agrawal DK. Transcriptional and epigenetic factors associated with early thrombosis of femoral artery involved in arteriovenous fistula. *Proteomes* 10 (2022): 14.
  62. Jin H, Goossens P, Juhasz P, et al. Integrative multiomics analysis of human atherosclerosis reveals a serum response factor-driven network associated with intraplaque hemorrhage. *Clin Transl Med* 11 (2021): 458.
  63. Chiorescu RM, Mocan M, Inceu AI, et al. Vulnerable atherosclerotic plaque: Is There a Molecular Signature? *International Journal of Molecular Sciences* 23 (2022): 13638.
  64. Rai V, Agrawal DK. Transcriptomic analysis identifies differentially expressed genes associated with vascular cuffing and chronic inflammation mediating early thrombosis in arteriovenous fistula. *Biomedicines* 10 (2022): 433.
  65. Chen Y, Qin Z, Wang Y, et al. Role of inflammation in vascular disease-related perivascular adipose tissue dysfunction. *Front Endocrinol (Lausanne)* 12 (2021): 710842.
  66. Samra G, Rai V, Agrawal DK. Innate and adaptive immune cells associate with arteriovenous fistula maturation and failure. *Can J Physiol Pharmacol* 100 (2022): 716-727.
  67. Samra G, Rai V, Agrawal DK. Heterogeneous population of immune cells associated with early thrombosis in arteriovenous fistula. *J Surg Res (Houst)* 5 (2022): 423-434.
  68. Fernandez DM, Giannarelli C. Immune cell profiling in atherosclerosis: role in research and precision medicine. *Nat Rev Cardiol* 19 (2022): 43-58.
  69. Eberhardt N, Giannarelli C. How single-cell technologies have provided new insights into atherosclerosis. *Arterioscler Thromb Vasc Biol* 42 (2022): 243-252.
  70. Alsaigh T, Evans D, Frankel D, et al. Decoding the transcriptome of calcified atherosclerotic plaque at single-cell resolution. *Commun Biol* 5 (2022): 1084.
  71. Yin Y, Xie Z, Chen D, et al. Integrated investigation of DNA methylation, gene expression and immune cell population revealed immune cell infiltration associated with atherosclerotic plaque formation. *BMC Med Genomics* 15 (2022): 108.
  72. Verma S, Kumar A, Narang R, et al. Signature transcriptome analysis of stage specific atherosclerotic plaques of patients. *BMC Med Genomics* 15 (2022): 99.
  73. Lowhalidanon K, Khunkaewla P. Discrimination between minimally modified LDL and fully oxidized LDL using monoclonal antibodies. *Anal Biochem* 619 (2021): 114103.
  74. Kubo T, Maehara A, Mintz GS, et al. The dynamic nature of coronary artery lesion morphology assessed by serial virtual histology intravascular ultrasound tissue characterization. *J Am Coll Cardiol* 55 (2010): 1590-1597.

75. Motreff P, Rioufol G, Finet G. Seventy-four-month follow-up of coronary vulnerable plaques by serial gray-scale intravascular ultrasound. *Circulation* 126 (2012): 2878-2879.
76. Nidorf SM, Fiolet AT, Mosterd A, et al. Colchicine in patients with chronic coronary disease. *New England journal of medicine* 383 (2020): 1838-1847.
77. Luo F, Das A, Chen J, et al. Metformin in patients with and without diabetes: a paradigm shift in cardiovascular disease management. *Cardiovasc Diabetol* 18 (2019): 54.

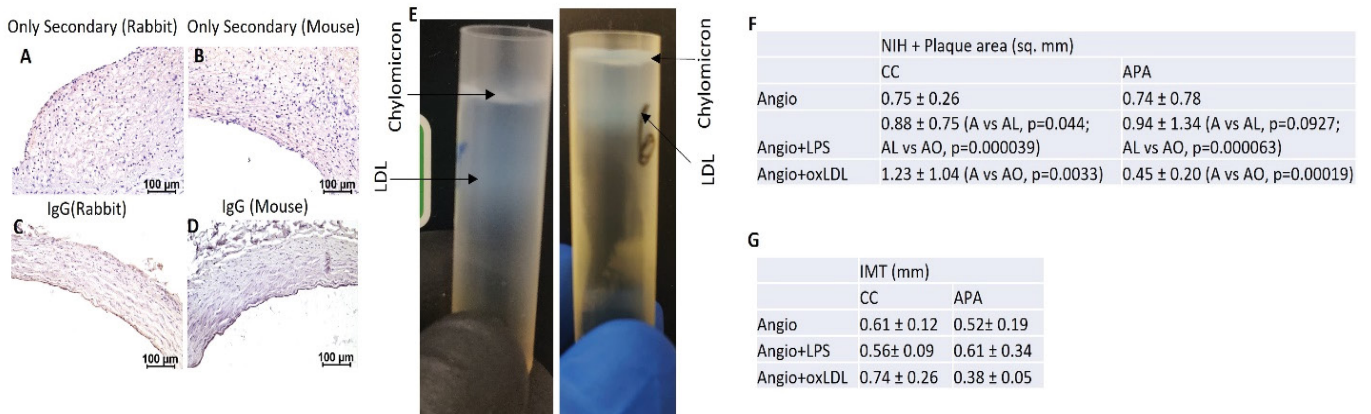


**Figure S1:** Control IgG and secondary only IHC stain, LDL preparation, neointimal hyperplasia + plaque area, and intimal-media thickness analyzed from H and E-stained sections. Secondary only without primary rabbit (panel A) and mouse (panel B), IgG controls (panels C and D), LDL preparation (panel E), neointimal hyperplasia (NIH) + plaque area (panel F), and intimal-media thickness (IMT; panel G)

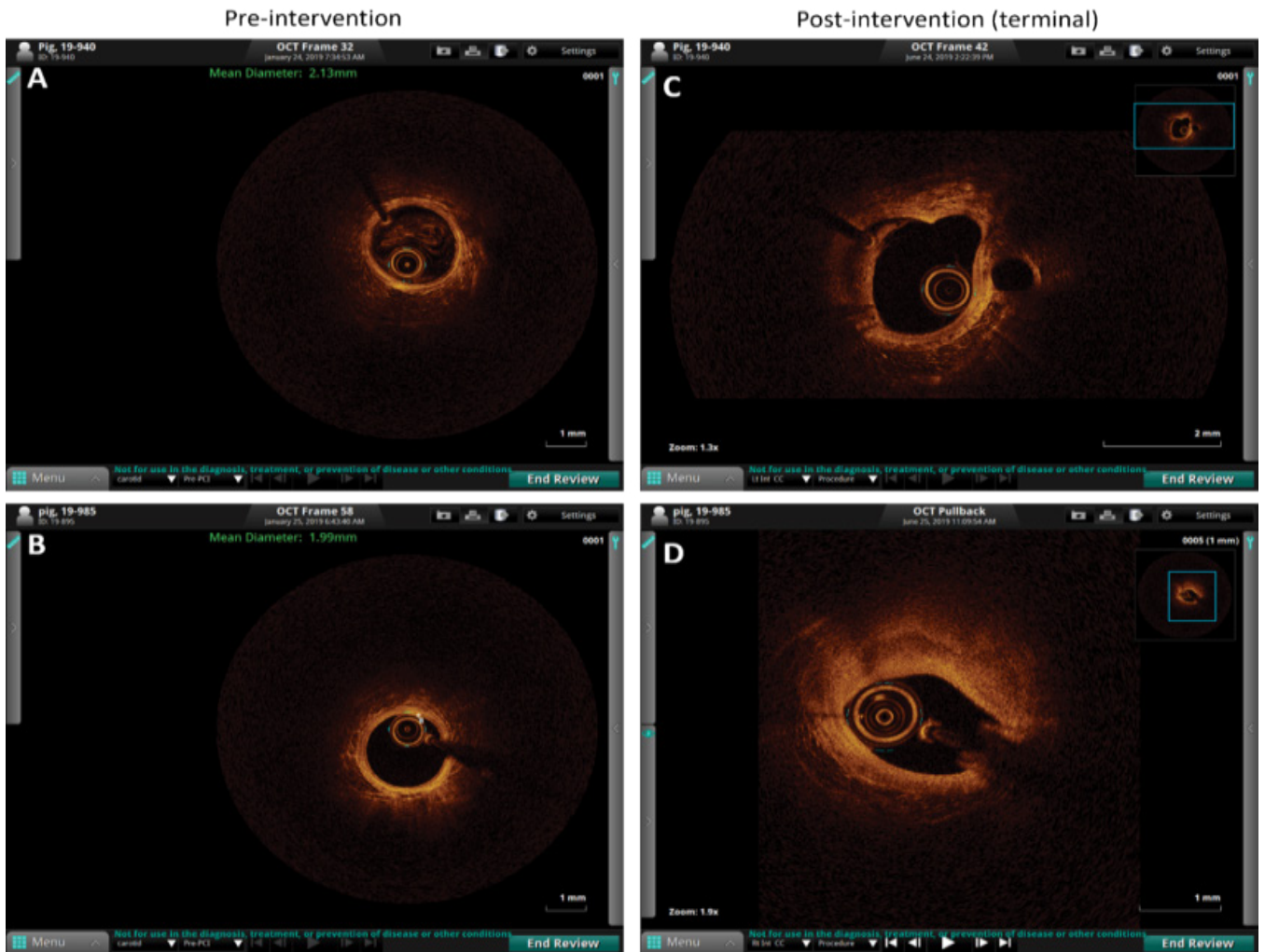


**Figure S2:** Optical Coherence Tomography (OCT) images from angioplasty + oxLDL group swine. Panels A and C- pre-intervention OCT and panels B and D- OCT images before sacrifice.

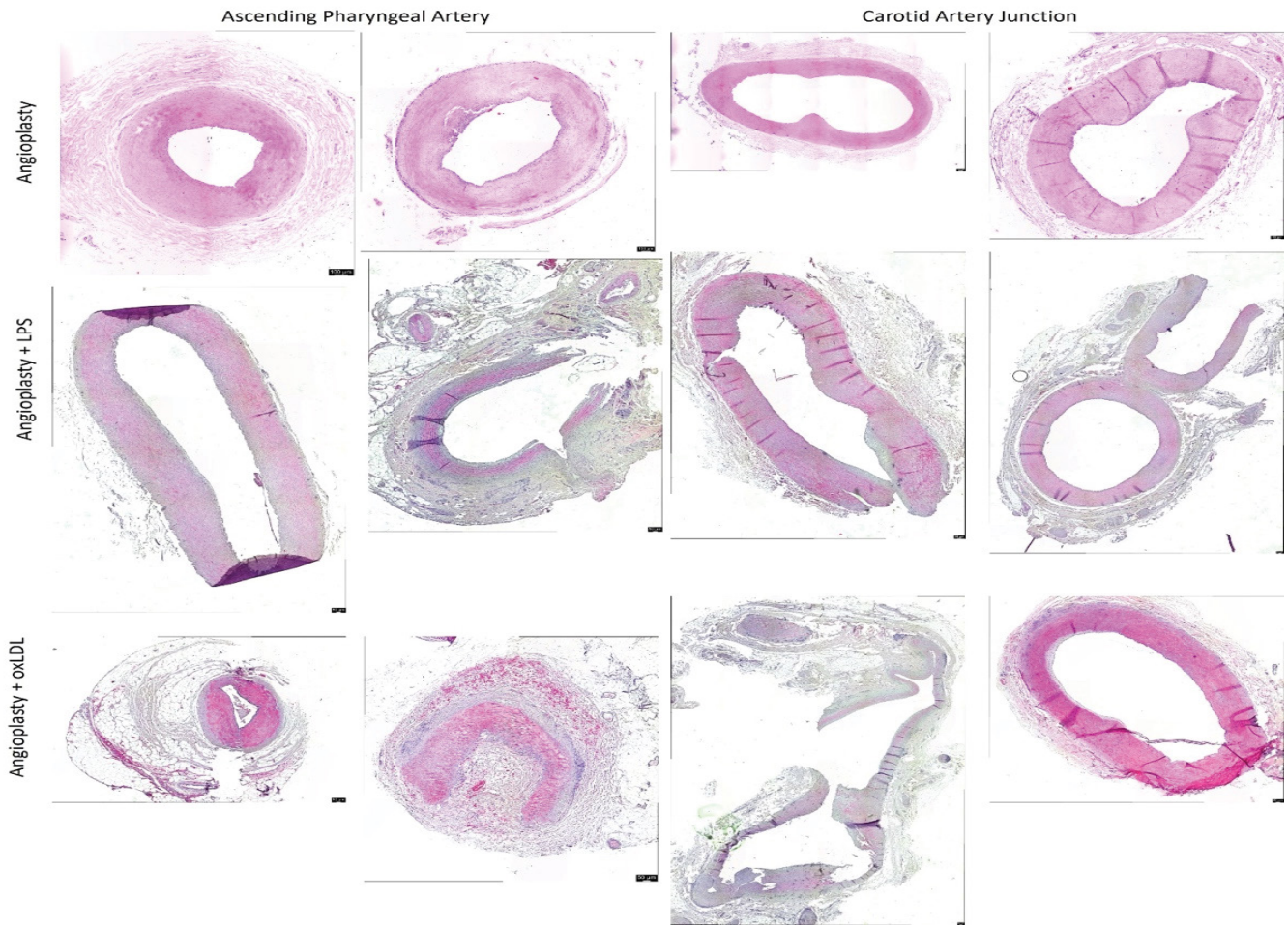


**Figure S3:** Hematoxylin and Eosin stain for ascending pharyngeal artery and carotid artery junction (area of intervention) for angioplasty, angioplasty + LPS, and angioplasty + oxLDL group swine.

**Table S1:** Criteria used to score Movat Pentachrome staining.

Score Stain	0	1	2	3	4	5
Collagen	Minimal yellow staining	Very weak yellow staining	Weak yellow staining	Moderate yellow staining	Strong yellow staining	Very strong yellow staining
Elastin	Minimal purple / black staining	Very weak purple / black staining	Weak purple / black staining	Moderate purple / black staining	Strong purple / black staining	Very strong purple / black staining
Fibrin	Minimal red staining	Very weak red staining	Weak red staining	Moderate red staining	Strong red staining	Very strong red staining
Glycans	Minimal blue staining	Very weak blue staining	Weak blue staining	Moderate blue staining	Strong blue staining	Very strong blue staining

**Table S2:** Movat-Pentachrome staining score in carotid junction and APA at the site of intervention. Lipopolysaccharide (LPS) and oxidized low-density lipoprotein (oxLDL).

Neointimal area and atherosclerotic lesion				
<b>Carotid Junction</b>				
	Collagen	Elastin	Glycans	Fibrin
Angioplasty alone	2-Jan	0-1	0-2	2-Jan
Angioplasty + LPS	2-Jan	3-Feb	3-Jan	3-Jan
Angioplasty + oxLDL	0-2	3-Feb	3-Jan	4-Jan
<b>APA</b>				
Angioplasty alone	3-Jan	0-1	1	3-Feb
Angioplasty + LPS	2-Jan	0-4	0-2	0-2
Angioplasty + oxLDL	0-1	0-2	0-2	2-Jan
Media and adventitia				
<b>Carotid Junction</b>				
	Elastin content			
Angioplasty alone	0-1	Near normal elastin staining		
Angioplasty + LPS	3-Jan	Increased elastin degradation in 1/3 to 1/2 media		
Angioplasty + oxLDL	5-Feb	Increased elastin degradation in 2/3 to entire media		
<b>APA</b>				
Angioplasty alone	0-1	Near normal elastin staining		
Angioplasty + LPS	4-Jan	Increased elastin degradation in 1/2 to entire media in all arteries		
Angioplasty + oxLDL	5-Jan	Increased elastin degradation in one artery		
		Medial hypertrophy with a constricted lumen in all arteries		